Development 140, 4362-4374 (2013) doi:10.1242/dev.098061

Semicircular canal morphogenesis in the zebrafish inner ear requires the function of *gpr126* (*lauscher*), an adhesion class G protein-coupled receptor gene

Fan-Suo Geng[1,*,‡], Leila Abbas[1,*], Sarah Baxendale[1,*], Celia J. Holdsworth[1], A. George Swanson[1], Krasimir Slanchev[2,§], Matthias Hammerschmidt[2,¶], Jacek Topczewski[3] and Tanya T. Whitfield[1,#]

SUMMARY

Morphogenesis of the semicircular canal ducts in the vertebrate inner ear is a dramatic example of epithelial remodelling in the embryo, and failure of normal canal development results in vestibular dysfunction. In zebrafish and *Xenopus*, semicircular canal ducts develop when projections of epithelium, driven by extracellular matrix production, push into the otic vesicle and fuse to form pillars. We show that in the zebrafish, extracellular matrix gene expression is high during projection outgrowth and then rapidly downregulated after fusion. Enzymatic disruption of hyaluronan in the projections leads to their collapse and a failure to form pillars: as a result, the ears swell. We have cloned a zebrafish mutant, *lauscher* (*lau*), identified by its swollen ear phenotype. The primary defect in the ear is abnormal projection outgrowth and a failure of fusion to form the semicircular canal pillars. Otic expression of extracellular matrix components is highly disrupted: several genes fail to become downregulated and remain expressed at abnormally high levels into late larval stages. The *lau* mutations disrupt *gpr126*, an adhesion class G protein-coupled receptor gene. Expression of *gpr126* is similar to that of *sox10,* an ear and neural crest marker, and is partially dependent on *sox10* activity. Fusion of canal projections and downregulation of otic *versican* expression in a hypomorphic *lau* allele can be restored by cAMP agonists. We propose that Gpr126 acts through a cAMP-mediated pathway to control the outgrowth and adhesion of canal projections in the zebrafish ear via the regulation of extracellular matrix gene expression.

KEY WORDS: Zebrafish, Adhesion GPCRs, *gpr126*, Inner ear, Semicircular canals, Extracellular matrix

INTRODUCTION

The three semicircular canals of the vertebrate inner ear detect angular acceleration (rotational movements) in three-dimensional space. Each canal consists of a curved fluid-filled duct, ending in a swelling or ampulla that houses a sensory organ: the crista. Formation of the semicircular canal ducts is a fundamental developmental process, involving the generation of form via movement and fusion of sheets of epithelium. In amniotes, flattened pouches form as outpocketings from the otic vesicle, and their apical sides touch and fuse to generate the semicircular canal ducts (Abraira et al., 2008; Chang et al., 2008) (reviewed by Bok et al., 2007). In a topologically equivalent process in anamniote vertebrates (zebrafish and *Xenopus*), the outpocketings are less pronounced, and finger-like projections of epithelium grow into the centre of the otic vesicle, where they fuse to form a pillar that becomes the hub of the canal (Waterman and Bell, 1984; Haddon and Lewis, 1991; Haddon and Lewis, 1996). Expression of *versican* (*vcan*) genes, which code for chondroitin sulphate proteoglycan core proteins, marks this process beautifully as it happens (Fig. 1).

Studies in the zebrafish, chick and mouse have begun to address the mechanisms underlying semicircular canal morphogenesis. It has been proposed that the cristae induce the ducts; signalling molecules, including Fgfs and Bmps, are likely to be involved (Cantos et al., 2000; Chang et al., 2004; Chang et al., 2008; Shawi and Serluca, 2008). Specification of canal tissue also requires the activities of various transcription factor genes, including *dlx5*, *hmx2/3*, *lmo4*, *otx1* and *sox10* (Hadrys et al., 1998; Acampora et al., 1999; Morsli et al., 1999; Fritzsch et al., 2001; Wang et al., 2001; Merlo et al., 2002; Wang et al., 2004; Lin et al., 2005; Hammond and Whitfield, 2006; Dutton et al., 2009; Deng et al., 2010).

Once canal projection or pouch tissue is specified, it must undergo morphological change to form the canal ducts. Outgrowth of projections in the *Xenopus* ear is driven by the production of the glycosaminoglycan hyaluronan (HA) (Haddon and Lewis, 1991). HA production in the zebrafish ear is regulated by *dfna5* (orthologue of the human autosomal dominant deafness gene *DFNA5*) and *ugdh* (*UDP-glucose dehydrogenase*), both expressed in the projections. In *dfna5* morphants and *jekyll* (*ugdh*) mutants, HA fails to be produced, and projection outgrowth is blocked (Neuhauss et al., 1996; Busch-Nentwich et al., 2004). Variable projection outgrowth defects in the zebrafish ear have also been reported after knockdown or mutation of *ncs1a* (Blasiole et al., 2005), *atrophin2* (*rerea* – Zebrafish Information Network), *fgf8a* (Asai et al., 2006), *cdh2* (Babb-Clendenon et al., 2006), *atp1a1a.2* (Blasiole et al., 2006), *atp2b1a* (Cruz et al., 2009) and *grhl2* (Han et al., 2011), and in Hedgehog pathway mutants (Hammond et al., 2010).

[1]MRC Centre for Developmental and Biomedical Genetics and Department of Biomedical Science, University of Sheffield, Sheffield, S10 2TN, UK. [2]Georges-Köhler laboratory, Max-Planck-Institute of Immunobiology, Freiburg, Germany. [3]Department of Pediatrics, Ann and Robert H. Lurie Children's Hospital of Chicago Research Center, Northwestern University Feinberg School of Medicine, Chicago, IL 60611-2605, USA.

*These authors contributed equally to this work
‡Present address: Brain and Mind Research Institute, Sydney Medical School, The University of Sydney, NSW 2006, Australia
§Present address: Max Planck Institute of Neurobiology, Am Klopferspitz 18, D-82152 Martinsried, Germany
¶Present address: Institute for Developmental Biology, Cologne University, D-50674 Köln, Germany
#Author for correspondence (t.whitfield@sheffield.ac.uk)

Accepted 9 August 2013

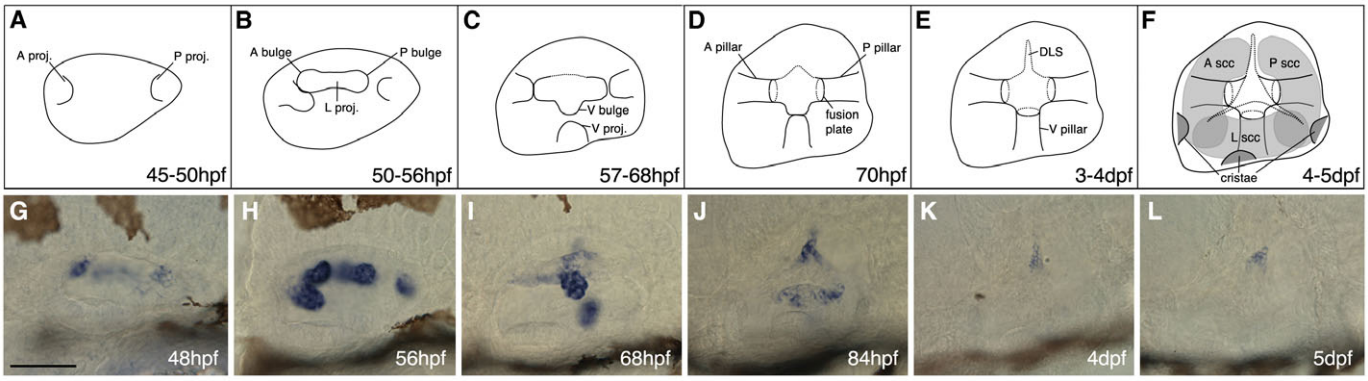

Fig. 1. Semicircular canal morphogenesis in the zebrafish ear. (A-F) Sketches of the developing semicircular canal system in the wild-type zebrafish ear, showing projection outgrowth, fusion and pillar formation. (G-L) Expression of *vcana* in the wild-type ear. (**A**,**G**) At 48 hpf, both anterior (A) and posterior (P) projections have begun to grow, and to express *vcana* at their tips. (**B**,**H**) The lateral projection, with its A and P bulges, is present by 50 hpf. The bulges and projections express *vcana* strongly at this time. The apparent downward growth of the A projection in H may be an artefact of fixation. (**C**,**I**) From 57-68 hpf, the A and P projections and bulges fuse to form the A and P pillars. The lateral projection now forms a ventral (V) bulge, and a V projection develops. Expression of *vcana* is downregulated in the A and P pillars, but is now strongly expressed in the V bulge and projection. (**D**,**J**) As fusion is completed at ~70 hpf, expression of *vcana* is downregulated in all pillars. Expression remains in the dorsolateral septum (DLS) at 84 hpf. (**E**,**K**) At 72 hpf, all three pillars are fused [timing of fusion was slightly later than previously reported (Waterman and Bell, 1984)]. (**F**,**L**) At 4-5 dpf, only a trace of *vcana* expression remains in the DLS. Grey shading indicates the canal lumens. The positions of the cristae are shown. Abbreviations: A, anterior; DLS, dorsolateral septum; P, posterior; proj., projection; ssc, semicircular canal; V, ventral. Scale bar: 50 μm.

When the sides of the canal pouches (in amniotes) or tips of the projections (in zebrafish and *Xenopus*) touch each other, cells change behaviour to form a fusion plate. Establishment of the zones of fusion and non-fusion in the mouse ear involves an antagonistic interaction between Lrig3 and Netrin1 (Salminen et al., 2000; Abraira et al., 2008), and regulation by Wnt signalling (Noda et al., 2012; Rakowiecki and Epstein, 2013). Resolution at the fusion plate in mouse, chick and *Xenopus* involves breakdown of the basal lamina (Haddon and Lewis, 1991; Salminen et al., 2000; Abraira et al., 2008), epithelial-to-mesenchymal transition (Salminen et al., 2000; Kobayashi et al., 2008) and cell death (Haddon and Lewis, 1991; Fekete et al., 1997; Cecconi et al., 2004). In the zebrafish, however, cell death does not appear to play a major role (Waterman and Bell, 1984; Fekete et al., 1997).

The mechanisms underlying these events – in particular how the growing projections recognize each other, adhere and fuse – are not fully understood. Here, we show that several extracellular matrix (ECM) components are expressed strongly in the epithelial projections in the zebrafish ear during outgrowth, and are then rapidly downregulated after fusion. We have characterized semicircular canal defects in a zebrafish mutant, *lauscher* (*lau*) (German: 'eavesdropper') (Whitfield et al., 1996). The *lau* mutant ear displays severe abnormalities in canal development: projections overgrow and fail to fuse correctly to form pillars. There are striking concomitant defects in the expression of ECM components in the canal projections, and the ear becomes swollen.

We show that *lau* mutations disrupt *gpr126*, an adhesion class G protein-coupled receptor (GPCR) gene. Adhesion GPCRs are one of five classes of GPCR, with dual roles in cell adhesion and signalling (Yona et al., 2008). These are exactly the functions that might be predicted to trigger changes in cell behaviour at the fusion plate. We show that the *lau* mutant ear phenotype can be ameliorated by treatment with cAMP agonists, indicating that Gpr126 is likely to signal through G protein-mediated activation of adenylyl cyclase and production of cAMP. The expression pattern of *gpr126* is very similar to that of *sox10*, and is partially dependent on Sox10 function. These data identify a new signalling mechanism involved in semicircular canal formation in the zebrafish, implicating Gpr126 in the control of projection outgrowth, contact recognition and fusion in the developing ear.

MATERIALS AND METHODS

Animals

Standard zebrafish husbandry methods were employed (Westerfield, 2000). Wild-type strains used were AB (ZDB-GENO-960809-7), WIK (ZDB-GENO-010531-2) and EKW (ZDB-GENO-990520-2); mutant alleles were lau^{tk256a} (ZDB-GENE-070117-2161), lau^{tb233c} (formerly bge^{tb233c}) (Whitfield et al., 1996), lau^{fr24} [isolated in the Hammerschmidt lab (Carney et al., 2010)] and lau^{vu39} (isolated in the Topczewski lab). Embryos of the *nac* ($mitfa^{w2/w2}$) strain (ZDB-GENO-990423-18), which lack melanophores (Lister et al., 1999), were used as wild types for some experiments. Embryos were raised in E3 (Westerfield, 2000) at 28.5°C. Work in Sheffield conformed to UK Home Office regulations.

Genetic mapping and sequencing

lau^{tb233c} homozygous adults (−/−) were crossed to the polymorphic WIK strain. Offspring of the heterozygous progeny (*tb233c*/WIK) were used for bulked segregant analysis. Six hundred and ninety-six mutant embryos from *tb233c*/WIK incrosses were used for fine mapping with SSLP and SNP markers. Candidate gene cDNA was generated using a SuperScript III First Strand Kit (Invitrogen). Sequencing was carried out using an ABI3730 capillary sequencer. Sequence data were analysed using FinchTV (www.geospiza.com); primers were designed using FastPCR (www.biocenter.helsinki.fi). Sequence numbering is given according to the NCBI reference sequence NM_001163291.1 (Monk et al., 2009).

Genotyping

Genomic DNA from mutant and wild-type embryos was amplified by PCR (see supplementary material Table S1 for primer sequences). The resulting *tb233c*, *tk256a* and *fr24* products were digested with the restriction enzymes *Sfa*NI, *Bsm*FI and *Bfa*I (New England Biolabs), respectively, for 5 hours at 37°C and separated on a 2% TBE agarose gel.

Morpholino injection

A morpholino oligonucleotide (Gene Tools) was designed to target the splice donor site of exon 19 of *gpr126*; a 5-base mismatch morpholino was used as a control (see supplementary material Table S1 for sequences).

Morpholinos were resuspended in water, and injected into one-cell stage embryos with 0.05% Phenol Red as described previously (Hammond and Whitfield, 2006).

Hyaluronidase injection

Wild-type embryos at 48-50 hours post-fertilization (hpf) were anaesthetized with tricaine (Sigma) and immobilized in 3% methylcellulose. *Streptomyces* hyaluronidase (Sigma) was dissolved at 0.5-1 mg/ml in PBS/0.5% Phenol Red; 1 nl was injected into the lateral projection of one ear, as described for *Xenopus* (Haddon and Lewis, 1991). Control injections were performed by injecting PBS/0.5% Phenol Red without hyaluronidase.

In situ hybridization

In situ hybridization was performed as described previously (Nüsslein-Volhard and Dahm, 2002). Probes used are listed in supplementary material Table S1. Embryos were bleached post-*in situ* where necessary in 0.5×SSC, 10% H_2O_2 and 5% formamide.

Immunohistochemistry

Embryos were fixed and dehydrated as for *in situ* hybridization. Following rehydration and washes in 1×PBS/0.1% Tween-20 (PBTw), samples were permeabilized with 20 μg/ml proteinase K (1 hour, room temperature) followed by PBTw washes. After blocking in 10% bovine serum, embryos were incubated overnight at 4°C in anti-collagen II antibody (1:500; II-II6B3; DSHB). After further washes and overnight incubation in anti-mouse IgG-HRP (Sigma), staining was visualized using the Vectastain DAB kit (Vector Labs).

Phalloidin staining

After fixation, embryos were rinsed in PBS and permeabilized in PBS/2% Triton-X100 (for 4 hours at room temperature). After PBS rinses, embryos were incubated overnight in 2.5 μg/ml FITC-phalloidin (Sigma) followed by PBS washes and mounting in Vectashield medium.

Drug treatment

Wild-type and homozygous *tb233c* mutant embryos were treated between 60 hpf (high pec) and 90 hpf with forskolin (Sigma; 2×6 hour pulses, 60-66 hpf and 84-90 hpf) at 25-100 μM or IBMX (3-isobutyl-1-methylxanthine) (Sigma; continuous treatment, 60-90 hpf) at 10-100 μM in E3. Control embryos were treated with equivalent amounts of DMSO (Sigma). To facilitate treatment times, embryos were incubated at 24°C from 8 hpf prior to drug treatment and at 28.5°C during treatments.

Microscopy and photography

Images were taken using an Olympus BX51 microscope, C3030ZOOM camera and CELLB software, and assembled with Adobe Photoshop. All panels are lateral views with anterior towards the left and dorsal towards the top, unless otherwise indicated.

RESULTS

The *lauscher* (*lau*) mutant has a defect in semicircular canal morphogenesis

The zebrafish *lauscher* (*lau*) mutant is characterized by its swollen ears at 5 days post-fertilization (dpf) (Fig. 2). We have analysed four alleles: two of these, lau^{tk256a} and bge^{tb233c}, were originally identified as separate loci (Whitfield et al., 1996). However, we have since shown that bge^{tb233c} is non-complementing and therefore allelic to *lau*. A third allele, *fr24*, isolated in a separate screen (Carney et al., 2010), was also allelic to *lau* by complementation testing (data not shown). A fourth allele, *vu39*, was also identified separately on the basis of its swollen ears.

At early stages of ear development in the *lau* mutant, otic patterning was normal (supplementary material Fig. S1), and sensory patches and otoliths developed correctly (Whitfield et al., 1996) (and data not shown). Initiation of semicircular canal formation was also normal: at 45 hpf, the anterior, posterior and lateral projections began to protrude into the otic vesicle. However, the projections subsequently failed to touch and fuse correctly (Fig. 2). The acellular core of the lateral projection often became enlarged, and did not form clear anterior, posterior and ventral bulges. In some individuals, the anterior and posterior projections continued to elongate, whereas in others, they ceased. The ventral projection also initially appeared to grow normally, but later also failed to fuse with the ventral bulge of the lateral projection. In some cases, the projections grew past one another (Fig. 2I); in the *tb233c* allele, projections occasionally touched and fused but did not

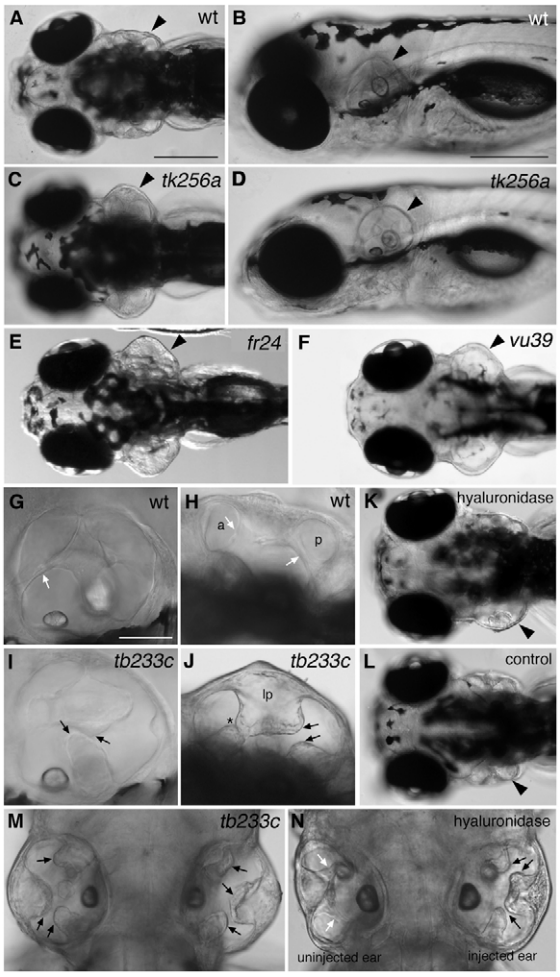

Fig. 2. *lauscher* mutant zebrafish have swollen ears at 5 dpf and defects in semicircular canal formation. (**A-F**) Live images of wild-type sibling (A,B) and homozygous mutant (C-F) embryos at 5 dpf. The ears (arrowheads) of the mutants are swollen at 5 dpf, but otoliths appear normal. (**G-J**) Live images of wild-type sibling (G,H) and *tb233c* mutant (I,J) ears at 5 dpf. (**K**) Injection of hyaluronidase into the lateral projection of the left ear of a wild-type embryo results in the collapse of the projection, failure of fusion and a swollen ear. (**L**) Injection of PBS into the lateral projection of the left ear has no effect on ear development. Arrowheads mark the injected ears. (**M**,**N**) Comparison of ear swelling and projection fusion in the *tb233c* allele (M) with an ear in which the lateral projection has been injected with hyaluronidase (N) (dorsal views). Black arrows mark unfused projections; white arrows mark fused pillars. Asterisk in J marks projections that have touched but not fused correctly. Abbreviations: a and p, lumens of anterior and posterior semicircular canals; lp, enlarged lateral projection. A,C,E,F,H,J-N are dorsal views. Scale bars: in A, 200 μm for A,C,E,F,K,L; in B, 200 μm for B,D; in G, 50 μm for G-J.

resolve to form a normal pillar (Fig. 2J). By the end of 3 dpf, the ears became swollen, most strongly in the *fr24* allele (Fig. 2E). Swelling in the *tb233c* allele was variable (see also Fig. 8).

Ear swelling in *lauscher* mutants is likely to result from failure of projection fusion

Endolymphatic hydrops of the mammalian inner ear is characteristic of a number of inner ear disorders (Everett et al., 2001; Hulander et al., 2003; Megerian et al., 2008). Initially, we hypothesized that the ear swelling in *lau* mutants might reflect this condition. However, the endolymphatic duct, a structure involved in the homeostatic regulation of endolymph, appeared to develop normally in the *lau* ear, as assayed by *bmp4* and *foxi1* expression (Fig. 3A-D). In addition, expression of *atp1a1a.4*, *kcnq1* and *nkcc1* (*slc12a2*) was normal or reduced (Fig. 3E-J). As these gene products have endolymph-generating functions (Lang et al., 2007; Abbas and Whitfield, 2009), a reduction in their levels is unlikely to explain the ear swelling. In addition, measurements of the perimeter and cross-sectional area of the ear suggested that the swelling was due to a shape change rather than indicating a significant increase in endolymph volume (supplementary material Fig. S2).

To test whether the loss of pillar formation might secondarily cause the swelling, we disrupted outgrowth of the projections with hyaluronidase, which is known to collapse the canal projections in the *Xenopus* ear (Haddon and Lewis, 1991). We injected hyaluronidase into the acellular space inside the lateral projection of one ear in wild-type embryos at 50 hpf, before fusion occurred. As in *Xenopus*, this blocked further projection outgrowth and fusion to form pillars, and at 5 dpf, 60% injected ears (18/30) were swollen (Fig. 2K-N). This was comparable with the degree of swelling in *tb233c* (Fig. 2M), but not as severe as in the other alleles. Control ears injected with a similar volume of PBS into the lateral projection did not swell (23/27 normal; four mildly swollen) (Fig. 2L). Taken together, these data suggest that the ear swelling in *lau* mutants is partly a secondary problem caused by a lack of projection fusion. However, we cannot rule out an additional effect on endolymph production or homeostasis (see Discussion).

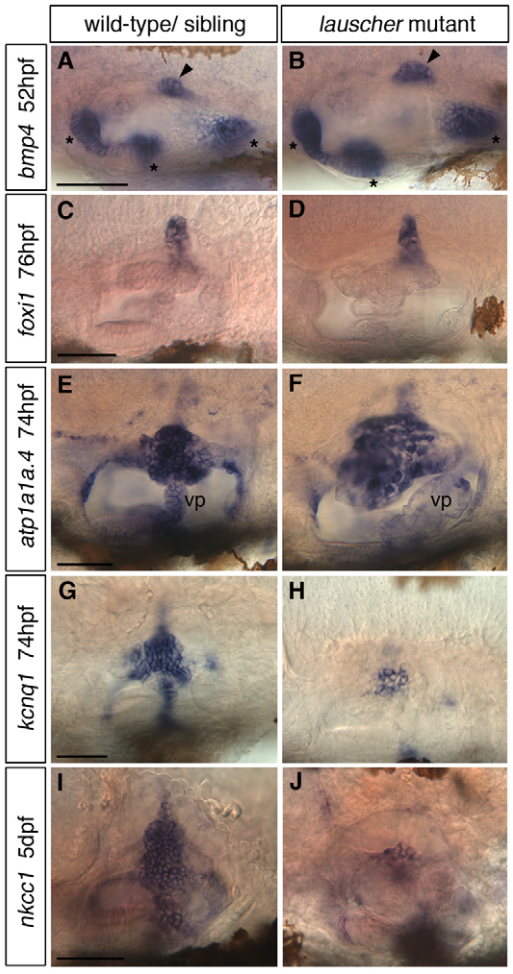

Fig. 3. Expression of genes involved in endolymph homeostasis in the *lau* mutant ear. (**A-D**) The endolymphatic duct, marked by expression of *bmp4* (arrowheads, A,B) and *foxi1* (C,D), appears to develop normally in *lau* mutants. The three cristae also express *bmp4* normally (asterisks, A,B). (**E-J**) Expression of ion transporter genes in the *lau* mutant ear. (E,F) Expression of the *atp1a1a.4* subunit of Na^+/K^+-*ATPase1* is more diffuse and lacking from the ventral pillar (vp). (G-J) There is a substantial reduction in both *kcnq1* and *nkcc1* expression. Abbreviation: vp, ventral pillar (E) or ventral projection (F). Alleles: B,D,H,J, *tk256a*; F, *tb233c*. Scale bars: 50 μm.

Expression of extracellular matrix genes and other markers is highly disrupted in the *lau* mutant ear

To characterize the semicircular canal defects further, we examined gene expression in the developing projections and pillars in the ear (Fig. 4). Most striking were changes in the expression of genes coding for extracellular matrix (ECM) proteins or ECM-modifying enzymes. Expression of the hyaluronan and proteoglycan link protein gene *hapln1a* persisted abnormally in the disorganized canal projections in *lau* mutants (Fig. 4A-F). Conversely, expression of *hapln3*, normally initiated as projections fused in wild-type embryos, was greatly reduced in *lau* mutants (Fig. 4G-L). The chondroitin sulphate proteoglycan core protein genes *versican a* (*vcana*) and *versican b* (*vcanb*) were expressed at high levels in the mutant unfused canal tissue, failing to be restricted to the dorsolateral septum as in the wild-type (Fig. 4M-X). There was precocious and ectopic accumulation of Type II Collagen protein in *lau* mutant canal tissue (Fig. 4Y-DD). Expression of the extracellular matrix synthesis enzyme genes *chondroitin synthase 1* (*chsy1*), *hyaluronan synthase 3* (*has3*) and *UDP-glucose dehydrogenase* (*ugdh*) was also upregulated in *lau* mutant ears (Fig. 4EE-JJ). In addition, we found substantial changes in the expression of other semicircular canal marker genes, including *aldh1a3*, *bmp7b* and *sox9b* (Fig. 4KK-PP).

Mutations in *lauscher* disrupt *gpr126*, a G protein-coupled receptor gene

We mapped *lau* to LG20 by bulked segregant analysis (Michelmore et al., 1991; Bahary et al., 2004). Six hundred and ninety-six mutant embryos from *tb233c*/WIK incrosses were used for fine mapping of the mutation to the region between SSLP markers Z4627 and Z536 (Fig. 5A). We narrowed this further to a region between SNP markers in *slc25a27* and *galnt14*. In this interval, a SNP marker was found in *schnurri2* for which there was no recombination event. There were six genes in the vicinity (Fig. 5A); of these, only *gpr126*, an adhesion class G protein-coupled receptor gene, was expressed in the inner ear (data not shown; see Fig. 6). We detected a number of alternatively spliced wild-type *gpr126* transcripts (data not shown).

Sequencing of *gpr126* cDNA and genomic DNA from the four *lau* mutant alleles indicated two missense mutations in the fourth

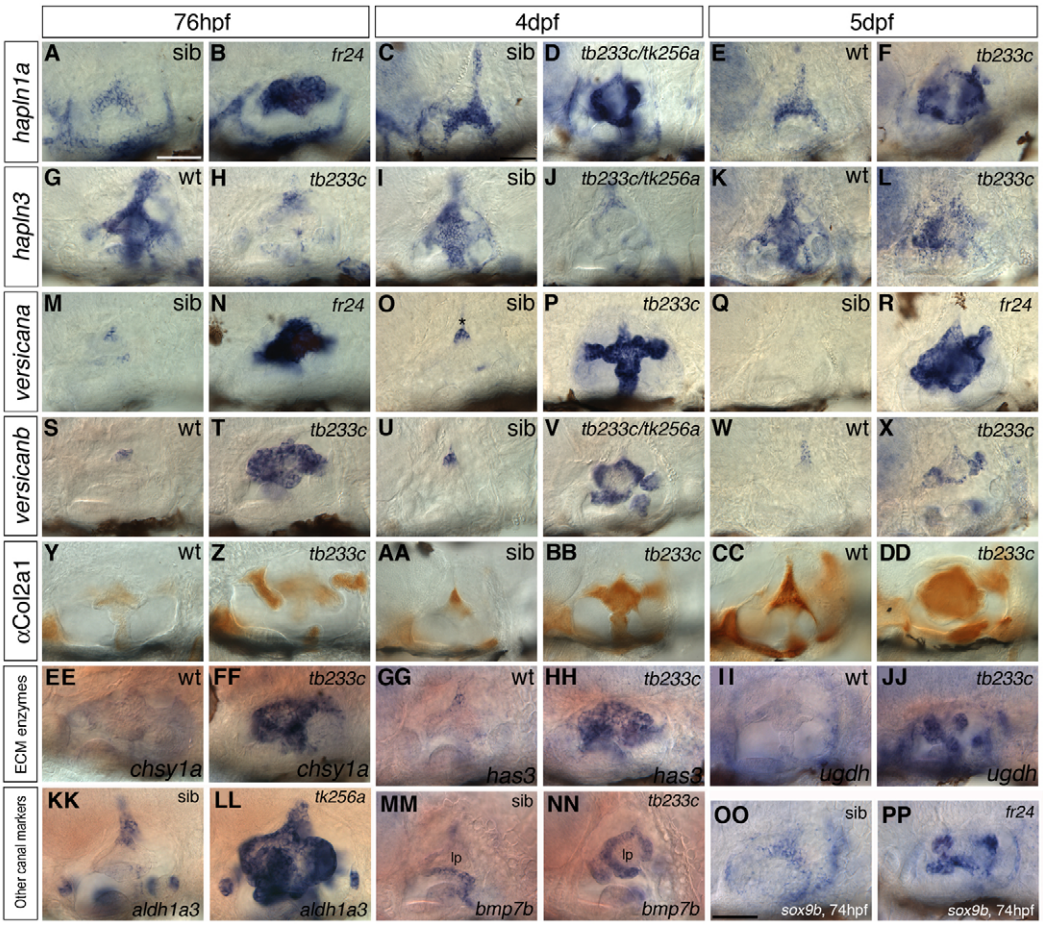

Fig. 4. Expression of extracellular matrix (ECM) genes and other semicircular canal markers is altered in the *lauscher* mutant ear. (**A-JJ**) Expression of ECM structural and enzyme genes in *lau* mutant ears at 76 hpf, 4 dpf and 5 dpf. Expression of the HA binding *hapln1a* (A-F) and the *versican* genes *vcana* and *vcanb* (M-X) is highly upregulated in mutant canal tissue. Expression of *hapln3* is normally upregulated in wild-type ears on canal projection fusion (G,I,K); in the mutant, fusion fails, and transcript levels remain low (H,J,L). Antibody staining for type II Collagen (Y-DD) shows precocious protein accumulation at 76 hpf in mutants (Y,Z), persisting at 4-5 dpf (AA-DD); aberrant canal tissue is visible. Genes coding for enzymes for chondroitin synthesis (*chsy1*, EE,FF) and HA production (*has3*, GG,HH; *ugdh*, II,JJ) are upregulated in mutants at 76 hpf. (**KK-PP**) The canal markers *aldh1a3*, *bmp7b* and *sox9b* are upregulated in the unfused projections in the *lau* mutant ear. wt, wild type; sib, phenotypically wild-type sibling. Mutant alleles are shown on the panels. Scale bars: in A, 50 μm (applies to columns 1 and 2); in C, 50 μm (applies to all other panels).

transmembrane domain, and two nonsense mutations predicting truncated proteins (Fig. 5B-D). In *tb233c* mutant embryos, a T→A transversion at position 2888 predicted the replacement of Ile963 (isoleucine) by asparagine. In *tk256a*, a C→T transition at position 2906 led to a replacement of the highly conserved proline Pro969 by leucine. In *fr24*, a T→A transversion at position 1388 resulted in a nonsense mutation at Leu463. In *vu39*, a G→A transition at position 2411 resulted in a nonsense mutation at Trp804 in the GPCR proteolytic site (GPS) motif, part of the recently described GAIN (GPCR autoproteolysis-inducing) domain (Araç et al., 2012). This tryptophan residue, which is highly conserved in GPS motifs from other adhesion GPCRs, was present in all wild-type cDNA variants that we isolated, but is reported as a cysteine in the reference sequence (Monk et al., 2009). In both nonsense alleles, the highly conserved CUB (Complement C1r/C1s, UEGF, BMP1) and PTX (Pentraxin) protein domains remained intact in the predicted truncated protein, but the GPS motif and 7-transmembrane (7TM) domain were lost (Fig. 5C). The sequence data indicated the loss or gain of restriction sites in three of the alleles, which we confirmed by genotyping (Fig. 5E).

To provide further confirmation of our sequence data, we used a morpholino to knock down *gpr126* function in wild-type embryos. This was designed to target the 19th exon, in which the first 7TM domain helix resides. Wild-type embryos injected with 5 ng of a five-mismatch control morpholino demonstrated normal semicircular canal formation (n=73). Embryos injected with 2.5 ng of the *gpr126* splice morpholino phenocopied both the morphological and gene expression defects in *lau* mutants, even though disruption of splicing was incomplete (Fig. 5F,G). As in *lau*, canal projections in the morphant ear failed to fuse or grew past one another. The knockdown of *gpr126* function persisted until 5 dpf and was dose dependent. A morpholino dose of 0.25 ng had no visible effect on the ear; at 1 ng, 40% injected embryos displayed *lau*-like ear defects (n=127), whereas at 2.5 ng (1 nl of 0.25 mM), 73% of injected embryos displayed *lau*-like ear defects (n=133). A 5 ng dose was toxic (data not shown). Sequence analysis indicated that the morpholino caused either skipping of exon 19 or the use of a cryptic splice site in exon 19 (Fig. 5G). In both cases, the reading frame of the mis-spliced transcript was shifted.

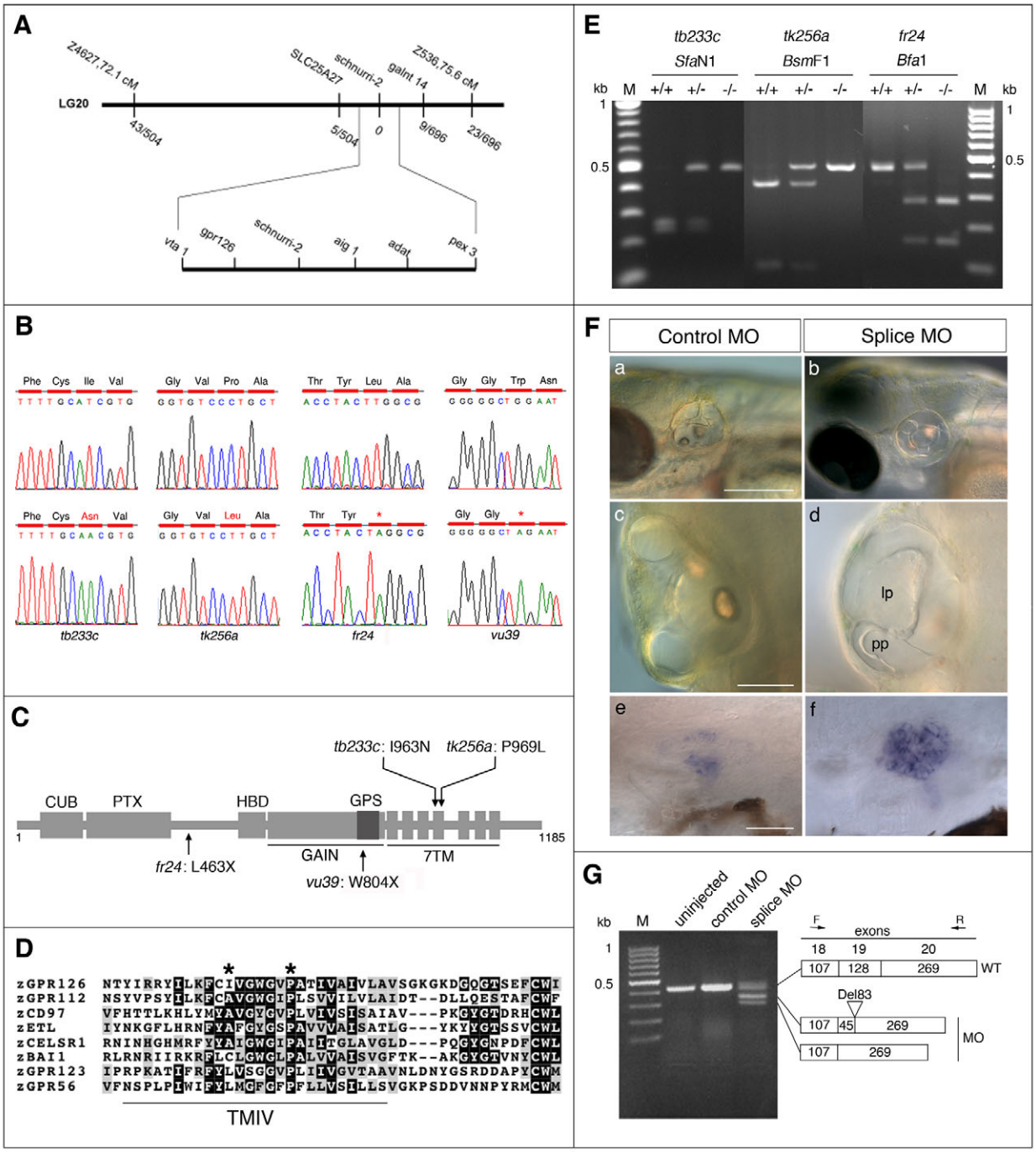

Fig. 5. Positional cloning, identification and confirmation of mutations in *gpr126*. (**A**) Genetic map of the *lau* locus. Numbers of meiotic recombinants for the flanking SSLP markers and SNP markers in *slc25a27*, *schnurri2* and *galnt14* are shown. (**B**) Sequence analysis of *gpr126* cDNA in wild type (upper panels) and *lau* mutants (lower panels), with predicted changes to the coding sequence. (**C**) Schematic diagram of the Gpr126 protein, with its conserved domains: CUB (Complement C1r/C1s, Uegf, BMP1), PTX (Pentraxin), HBD (hormone binding domain), GAIN (GPCR autoproteolysis inducing) domain, GPS (GPCR proteolytic site) motif and 7TM (7-transmembrane) domain (not to scale). Positions of the mutations are shown. (**D**) Amino acid comparison of the fourth transmembrane (TMIV) region from eight zebrafish adhesion class GPCRs, showing the conserved hydrophobic residue at position 963 (mutated in *tb233c*), and the highly conserved proline (P) at position 969 (mutated in *tk256a*) (asterisks). (**E**) Genotyping of *lau* mutant fish by restriction digest of PCR-amplified genomic DNA. In *tb233c*, the mutation eliminated an *Sfa*N1 site; in *tk256a*, the mutation eliminated a *Bsm*F1 site; in the *fr24* allele, a *Bfa*1 site was gained. (F,G) *gpr126* morpholino injection recapitulates the *lau* mutant ear phenotype. (**F**) Wild-type (*nac*) embryos (left hand panels) injected with 5 ng control morpholino exhibit normal ear morphology at 5 dpf (a,c), and low *vcanb* expression at 5 dpf (e). Wild-type (*nac*) embryos injected with 5 ng *gpr126* morpholino (right hand panels) have abnormal projection outgrowth (b,d). The lateral projection (lp) is enlarged, and the posterior projection (pp) in this ear has grown past the lateral projection without fusing. Expression of *vcanb* is upregulated (f). (**G**) RT-PCR analysis of *gpr126* mRNA processing of the 19th exon in *gpr126* morpholino-injected, or in control (mismatched) morpholino-injected, embryos at 5 dpf. Sequencing confirmed two aberrant splice variants. Panels c,d are dorsal views, anterior towards the top. Scale bars: 200 μm in a,b; 50 μm in c,d; 50 μm in e,f.

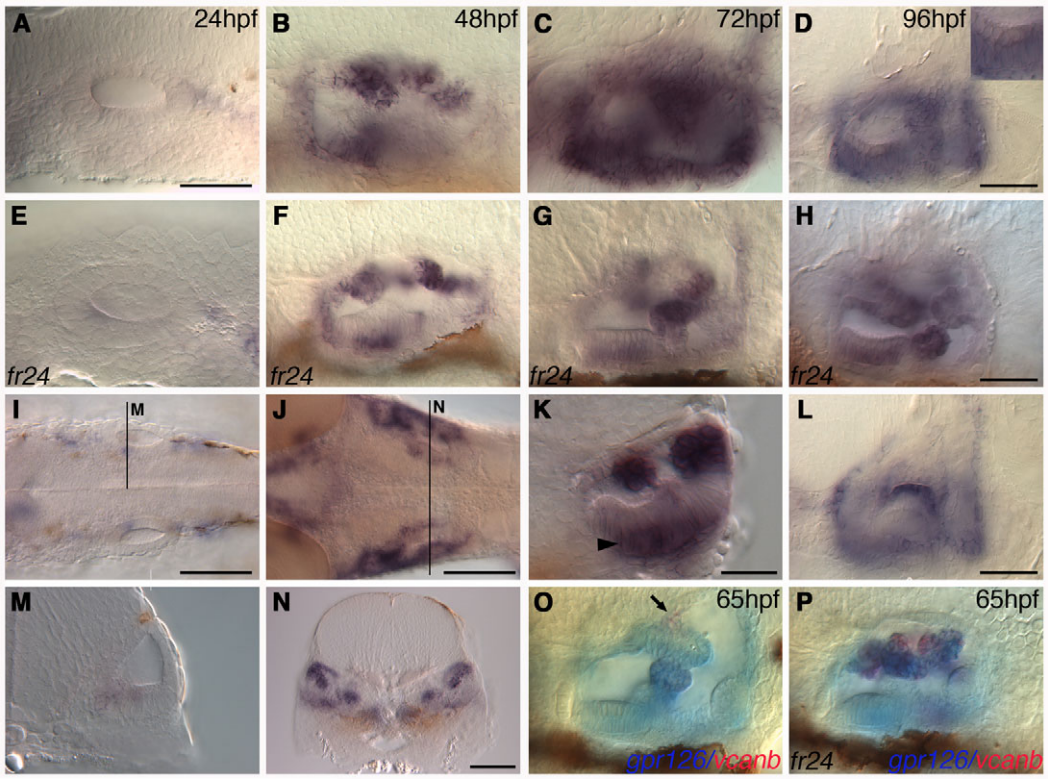

Fig. 6. Expression of *gpr126* in wild-type and *lauscher* mutant ears. (**A-H**) Expression of *gpr126* mRNA in the ear at 24-96 hpf in wild-type (A-D) and *fr24* mutant embryos (E-H). Strongest expression is in canal projections prior to fusion (48-72 hpf), with some expression remaining at 96 hpf. Inset in D: higher magnification showing expression in the anterior macula supporting cell layer. (**I**,**M**) Wild-type expression of *gpr126* at 26 hpf in the anterior macula (I, dorsal view; M, transverse section). (**J**,**N**) Expression at 48 hpf shows stronger staining in the projections and sensory patches (J, dorsal view; N, transverse section). (**K**) Expression in sensory patches at 72 hpf is restricted to supporting cells (arrowhead) (transverse section; see also inset in D). There is strong expression in the projections. (**L**) Alternative focus view of D, showing residual expression in the lateral projection at 96 hpf. (**O**,**P**) Expression of *gpr126* (blue) and *vcanb* (red) in the projections of wild-type and *fr24* mutant embryos at 65 hpf. In wild-type embryos (O), there is co-expression (purple) in the recently fused ventral pillar; *vcanb* is downregulated in the lateral projection and in the anterior and posterior pillars (out of focus), whereas *gpr126* is expressed at reduced levels. In *fr24* mutants (P), *vcanb* and *gpr126* are co-expressed in the unfused projections. Expression of *vcanb* persists in the dorsolateral septum, which does not express *gpr126*, in both wild-type and mutant embryos (O, arrow). Scale bars: in A, 50 μm for A-C,E-G,M,O,P; 50 μm in D,H,L; 25 μm in K; 100 μm in I,J,N.

The degree of ear swelling in the *lau* alleles correlated well with the predicted disruption of protein function. Both *tb233c* and *tk256a* (missense mutations) showed a milder and more variable ear swelling than the *fr24* allele, which has a truncating mutation (Figs 1, 5, 8). Two further alleles of zebrafish *gpr126*, isolated in a screen for myelination defects, have been described (Pogoda et al., 2006; Monk et al., 2009). We found that our alleles also displayed a reduction or loss of *myelin basic protein* (*mbp*) expression in the posterior lateral line nerve and ganglion at 5 dpf, the degree of which also correlated well with the predicted strength of the alleles (supplementary material Fig. S3). We conclude that *tb233c* and *tk256a* are hypomorphic alleles, with *tb233c* the weaker of the two, whereas *fr24* and *vu39* are stronger, possibly null, alleles.

gpr126 mRNA is strongly expressed in the developing semicircular canal projections

A striking aspect of the *gpr126* expression pattern was in the developing ear (Fig. 6; supplementary material Fig. S4). A trace of expression was seen in the otic vesicle at 24 hpf (Fig. 6A,I,M), and strong expression appeared in the canal projections as they grew out at 48 hpf (Fig. 6B-D,J,K,N). *gpr126* was also expressed in the supporting cells of the anterior macula (Fig. 6D,K). Expression levels were similar in both wild-type and *lau* mutant embryos (Fig. 6E-H); however, expression in *lau* persisted at slightly higher levels in the unfused projections at 96 hpf (Fig. 6H). In the canal projections, expression overlapped with that of *vcanb* at the projection tips, but *gpr126* expression was more widespread (Fig. 6O,P). After projection fusion in wild-type embryos, *gpr126* expression persisted in the pillars at lower levels, whereas *vcanb* was no longer detectable in the pillars (Fig. 6O). Otic expression of *gpr126* decreased in both wild-type and mutant embryos at later stages (not shown).

Expression of *gpr126* in *colourless* (*sox10*) mutants is lost in the ear and in neural crest-derived glia

In addition to its expression in the ear, *gpr126* was expressed dynamically in other tissues during early development (Fig. 7; supplementary material Fig. S4). We detected *gpr126* expression in neural crest-derived glia, mesoderm, heart, olfactory epithelium, and head and pectoral fin chondrocytes. This expression pattern was very similar to that of *sox10*, a SoxE family transcription factor gene expressed in the neural crest and ear (Fig. 7A-D) (Dutton et al., 2001; Dutton et al., 2009). This led us to ask whether Sox10 regulated *gpr126* expression. In *colourless* (*cls*) (*sox10*$^{-/-}$) mutants at 24 hpf, *gpr126* was specifically missing from a group of cells

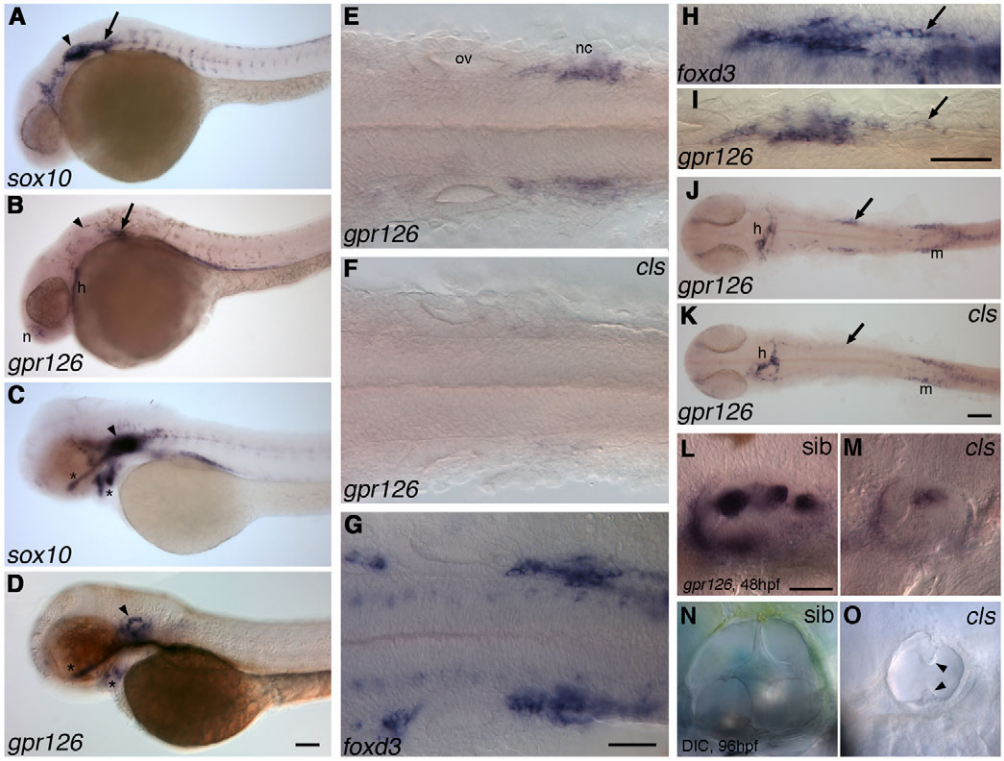

Fig. 7. Comparison of expression of *gpr126* and *sox10* in wild-type embryos, and expression of *gpr126* in *colourless* (*sox10*$^{-/-}$) mutant embryos. (**A-D**) Expression of *gpr126* and *sox10* in wild-type embryos at 24 hpf (A,B) and 48 hpf (C,D). Both genes are expressed in the otic vesicle (arrowhead), post-otic region (arrow), olfactory epithelium (nose, n) and head chondrocytes (asterisks). (**E-G**) Dorsal views of flat-mounted 24 hpf embryos: post-otic expression of *gpr126* in the wild type (E) is lost in the *cls* mutant (F). Comparison with *foxd3* expression identifies these cells as neural crest (G). (**H**,**I**) Dorsal view of the post-otic region showing *foxd3*-expressing Schwann cells extending posteriorly (H, arrow) and expression of *gpr126* in the same location (I, arrow). (**J**,**K**) *gpr126* expression in heart (h) and posterior mesoderm (m) persists in *cls* mutants, whereas neural crest expression is lost (arrows). (**L**,**M**) Expression of *gpr126* is reduced in the *cls* mutant ear at 48 hpf, with weak expression in rudimentary projections (M). (**N**,**O**) DIC images of live ears at 96 hpf, showing a representative *cls* mutant ear (O). Note the small overall size and rudimentary unfused canal projections (arrowheads). Abbreviations: h, heart; m, posterior mesoderm, n, nose (olfactory epithelium); nc, neural crest; ov, otic vesicle; sib, phenotypically wild-type sibling embryo. Scale bars: in D, 100 µm for A-D; in G, 50 µm for to E-G; in I, 50 µm for H,I; in K, 100 µm for J,K; in L, 50 µm for L-O.

posterior to the otic vesicle (Fig. 7E,F,J,K). Comparison with expression of *foxd3*, a neural crest marker (Odenthal and Nüsslein-Volhard, 1998; Kelsh et al., 2000), confirmed that these were Schwann cells associated with the posterior lateral line ganglion and nerve (Fig. 7E-I). This fits with the known requirement for Gpr126 in the initiation of myelination by Schwann cells (Monk et al., 2009; Monk et al., 2011; Glenn and Talbot, 2013). As *foxd3*-expressing glia are reduced but still present at 27 hpf in *cls* mutants (Kelsh et al., 2000), the complete loss of *gpr126* expression in these cells at 24 hpf indicates that *gpr126* expression here is *sox10* dependent. In the *cls* mutant ear, expression of *gpr126* was also severely downregulated, even in ears containing rudimentary epithelial projections (Fig. 7L-O). Expression of *gpr126* in the heart and posterior mesoderm appeared to be independent of Sox10 function (Fig. 7J,K).

Application of cAMP agonists results in partial rescue of semicircular canal pillar formation in hypomorphic mutant *lau* embryos

Many GPCRs bring about their downstream effects via cAMP signalling (Jalink and Moolenaar, 2010) (and references within). Forskolin, which activates adenylyl cyclase and raises intracellular cAMP levels (Seamon and Daly, 1981), has been shown to rescue the myelination defect in *gpr126*^{st49} mutants (Monk et al., 2009). To show whether increased cAMP could also rescue the ear defects in *lau,* we applied two agonists of cAMP signalling to mutant embryos. In addition to forskolin, we used IBMX, which acts as a competitive, non-selective phosphodiesterase inhibitor to raise intracellular cAMP and cGMP levels and activate PKA (Schultz et al., 1973; Elks and Manganiello, 1985). Forskolin and IBMX can each act on other pathways, but their only common target is cAMP.

Both forskolin and IBMX were found to ameliorate the ear phenotype in *tb233c* embryos when applied during a crucial window of ear development spanning 60-90 hpf (Fig. 8; supplementary material Fig. S5). The extent of ear swelling was assayed visually in a dorsal view and categorized as ‘not swollen’, ‘mild’ or ‘severe’. Treatment with DMSO alone had no significant rescuing effect (Fig. 8M-P,CC). However, treatment with either forskolin (Fig. 8Q-T) or IBMX (Fig. 8U-X) resulted in a significant rescue of the *tb233c* allele, reducing swelling (compare Fig. 8D,X) and *vcan* expression (Fig. 8Y-BB), and restoring fusion and pillar formation (asterisks, Fig. 8T,X; supplementary material Fig. S5). The rescue was dose dependent (Fig. 8CC; supplementary material Fig. S5). Pillar formation was not perfect, however, with occasional small protrusions of tissue present on the fused pillars (arrowheads, Fig. 8T,X; supplementary material Fig. S5). In the stronger *fr24* allele, forskolin was effective, but IBMX treatment resulted in only a partial rescue (data not shown). Interestingly, we also found that incubation at a

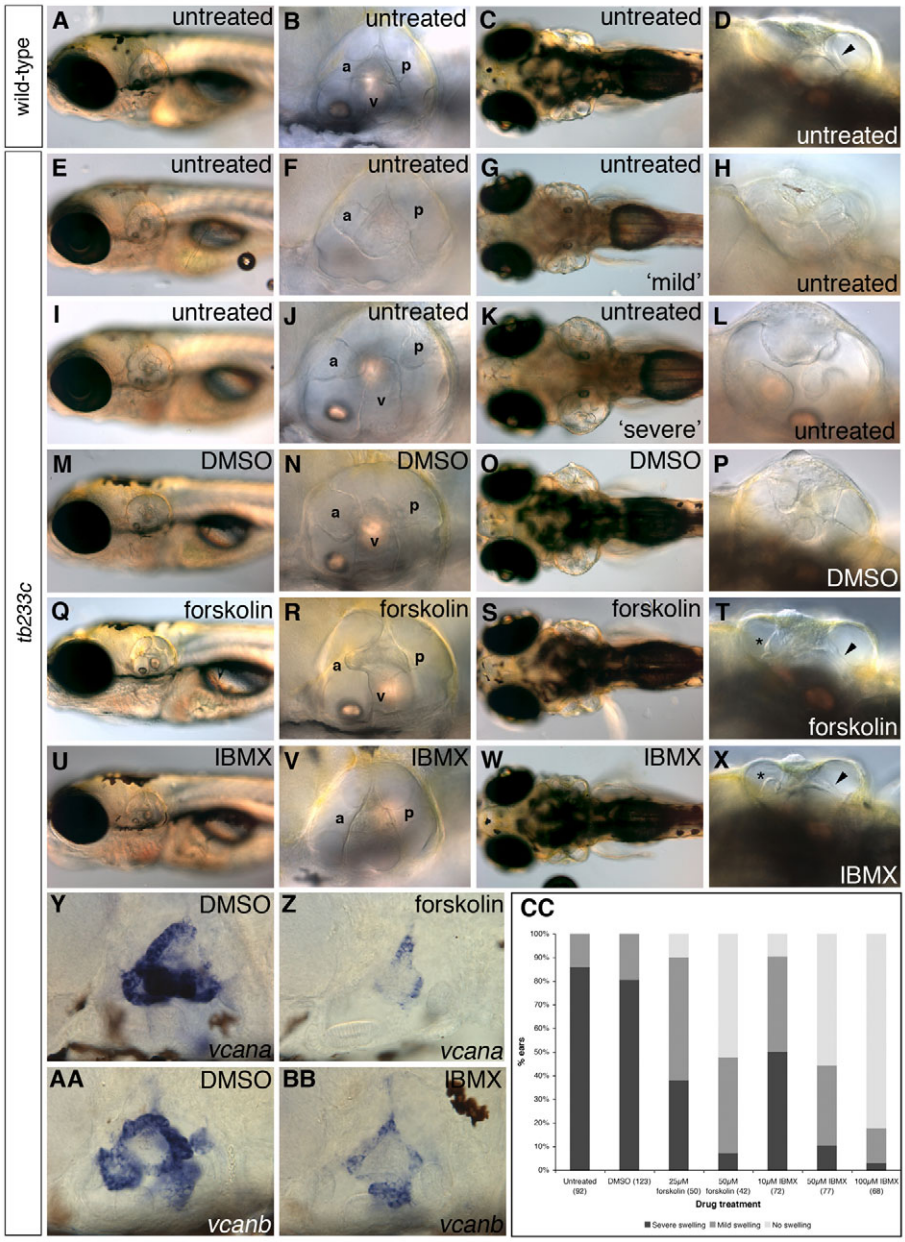

Fig. 8. Treatment with cAMP agonists rescues the *lauscher* ear phenotype. (**A-X**) Live images at 5 dpf in control and drug-treated embryos. Ear swelling in *tb233c* mutants was variable, and categorized as 'mild' (E-H) or 'severe' (I-L) compared with wild type (A-D). Arrowhead in D indicates fused pillar in the untreated wild-type ear. Treatment between 60 and 90 hpf with cAMP agonists forskolin (25 μM; Q-T) and IBMX (100 μM; U-X) rescues the swollen ear phenotype; DMSO has no effect (M-P). Fusion of the anterior (a), posterior (p) and ventral (v) projections to form pillars is also restored: rescued pillars are present in drug-treated embryos (R,V; arrowheads in T,X) but not in DMSO-treated samples (N,P). However, small, ectopic tissue protrusions are present on the rescued pillars (asterisks, T,X). (**Y-BB**) Both drugs (forskolin, 50 μM; IBMX, 100 μM) can reduce expression of *vcan* genes in the ear (Y-BB). (**CC**) Graphical representation of the ear swelling data, analysed with a 3×3 (DMSO, forskolin) or 3×4 (DMSO, IBMX) chi-square contingency table; $P<0.001$ (both drugs). *n* values are in parentheses. (C,G,K,O,S,W) Dorsal views.

lower temperature throughout the fusion period had a partial rescuing effect in the *tb233c* allele (supplementary material Fig. S6).

However, if cAMP agonists were applied to wild-type embryos over the same 60-90 hpf time window, high doses also induced an ear swelling when compared with DMSO controls, which could reflect a direct cAMP-mediated stimulation of endolymph production (supplementary material Fig. S7; see Discussion). Fusion was also disrupted, and expression of *vcana* remained high in any unfused projections, suggesting that there may be an additional contact-mediated requirement for its transcriptional downregulation.

DISCUSSION

Regulation of zebrafish semicircular canal morphogenesis by Gpr126, an adhesion class G protein-coupled receptor

Formation of semicircular canals in the zebrafish ear requires outgrowth of epithelial projections, contact recognition, adhesion and formation of a fusion plate, resulting in pillars of tissue spanning the otic vesicle. We have shown here that an orphan adhesion class G protein-coupled receptor gene, *gpr126*, is expressed in the outgrowing projections of the zebrafish ear, and that its function is required for correct fusion plate and pillar formation. This fits well with the proposed roles of other adhesion class GPCRs in adhesion, signalling and cell-cell or cell-matrix interactions (Bjarnadóttir et al., 2004; Bjarnadóttir et al., 2007; Yona et al., 2008).

The 7-transmembrane (7TM) region in adhesion class GPCRs tends to be divergent from that of other GPCRs, and has been functionally implicated in cellular migration and dimerization of the protein [(Yona et al., 2008) and references within]. The two missense mutations in the *tk256a* and *tb233c* alleles suggest that this region, and especially TMIV, is important for Gpr126 function. In particular, the substitution in *tk256a* of Pro969, which is highly conserved throughout all adhesion GPCRs (Bjarnadóttir et al., 2004; Bjarnadóttir et al., 2007), may affect insertion of the protein into the membrane or disrupt function.

The partial rescue of pillar formation in hypomorphic *lau* mutants by artificial elevation of cAMP levels indicates that Gpr126 signalling in the ear is mediated through a cAMP/Protein Kinase A pathway, as previously shown for Schwann cell myelination (Monk et al., 2009). As rescue of the ear phenotype was not efficient in the stronger *fr24* allele, this is still consistent with a putative role for the extracellular domain of the protein in mediating contact or adhesion at the fusion plate. The rescue data also suggest that Gpr126 functions through association with a stimulatory G protein alpha subunit ($G\alpha_s$), although this has not yet been identified. Three $G\alpha_s$ genes have been identified in the zebrafish genome, and a fourth gene belonging to a novel class of G alpha subunit, *gnav1*, is expressed in the inner ear (Oka et al., 2009). These four genes are potential candidates for the Gα subunit that interacts with Gpr126.

Gpr126 function is required for the normal expression of various ECM genes in the semicircular canal projections

In the *lau* mutant ear, we found dramatic alteration of expression of genes coding for ECM core proteins or modifying enzymes, suggesting that Gpr126 signalling is required directly or indirectly for their regulation. Outgrowth of the canal projections in *Xenopus* and zebrafish is driven by ECM production, in particular of the glycosaminoglycan hyaluronan (HA) (Haddon and Lewis, 1991; Busch-Nentwich et al., 2004) (and this work). We have shown here that other ECM components are expressed dynamically in zebrafish canal projections, including chondroitin sulphate proteoglycans (CSPGs) and proteoglycan link proteins, where they might influence both the mechanical and signalling properties of the projections. This correlates with the observation that the epithelial cells of the growing projections are rich in rough endoplasmic reticulum, indicating active protein synthesis (Waterman and Bell, 1984). In the dysmorphic, unfused canal projections of the *lau* mutant ear, expression of several ECM genes remains at high levels, suggesting that the projections remain in an 'outgrowth-like' state, and fail to undergo the normal changes associated with fusion and pillar formation. We infer that Gpr126 normally provides the signal that triggers this change in cell behaviour.

The persistence of *vcan* (a CSPG core protein gene) and *chsy1* (*chondroitin synthase*) expression in the unfused projections of the *lau* mutant ear is of considerable interest. Versicans interact with a range of ECM and cell-surface components, including both HA (via link proteins) and EGFR. They are generally known to be anti-adhesive molecules, and are upregulated in a number of malignant tumours (reviewed by Ricciardelli et al., 2009). Regulation of *versican* expression and/or processing is known to be essential for mammalian palate fusion (Enomoto et al., 2010) and cardiac ventricular septal formation (Hatano et al., 2012), both of which require fusion and remodelling events similar to those found in semicircular canal pillar formation. In *Xenopus*, immunoreactivity to chondroitin sulphate (CS) is high on the epithelium of the semicircular canal projections in the ear, but is absent from the core of the projections (Haddon and Lewis, 1991). Interestingly, CS is a ligand for two human adhesion class GPCRs, EMR2 and CD97 (Stacey et al., 2003; Kwakkenbos et al., 2005). Morpholino-mediated knockdown of *chsy1*, or overexpression of human *CHSY1* mRNA in the zebrafish, disrupts canal pillar formation, but leaves development of sensory cristae intact (Li et al., 2010).

Fused pillars are likely to provide structural support in the ear

The otic swelling in *lau* mutants appears to be, at least in part, a secondary consequence of the failure of projection fusion, rather than its cause. We have shown that the ears swell when canal projection outgrowth is disrupted by genetic, enzymatic or chemical means. A similar ear swelling is seen in *dfna5* morphants (Busch-Nentwich et al., 2004), where there is insufficient production of ECM and a lack of projection outgrowth, rather than overgrowth and failure of fusion as in *lau* mutants. We propose that any process that causes the failure of fusion, whether an overgrowth or an agenesis of the projections, can lead to ear swelling. This might be due to a lack of physical support that would normally counteract turgor pressure from the endolymph. It is also possible that the hygroscopic properties of both Versican and HA (Chen and Abatangelo, 1999; Wight, 2002) act to draw fluid into the otic vesicle, which might contribute to swelling in *lau* mutant ears.

An alternative explanation is a disruption to endolymph homeostasis. Although we did not find direct evidence to support this conclusion, semicircular canal duct epithelium is known to be an endolymph-generating tissue (Milhaud et al., 2002; Abbas and Whitfield, 2009; Pondugula et al., 2013), and so any defects in canal tissue might have secondary effects on endolymph production. cAMP signalling can stimulate endolymph production directly (e g. Sunose et al., 1997a; Sunose et al., 1997b; Milhaud et al., 2002; Pondugula et al., 2013), which could explain the swelling seen after treatment of wild-type ears with cAMP agonists.

Potential conservation of Gpr126 function in the ear

Morphogenesis of the semicircular canal system shows both similarities and differences between amniotes and anamniotes. In the chick and mouse, flattened pouches are formed from the otocyst, rather than finger-like projections: it is the sides of these pouches, rather than the tips of the fingers, that recognize and fuse with each other (Martin and Swanson, 1993; Bissonnette and Fekete, 1996). The resultant fusion plate is thus much larger than that in *Xenopus* or zebrafish, and cell death is thought to be the primary mechanism for clearance of cells in this region, at least in the chick (Fekete et al., 1997; Lang et al., 2000; Cecconi et al., 2004; Kobayashi et al., 2008). In addition, the *dfna5*/*ugdh*/HA pathway, which is implicated in semicircular canal projection outgrowth in the fish, does not appear to be conserved in the mouse (Busch-Nentwich et al., 2004; Van Laer et al., 2005). By contrast, other genes involved in canal formation, such as *Otx1*, are highly conserved between fish and mammals (Hammond and Whitfield, 2006). Despite the differences, formation of the canal ducts in all groups requires the recognition, adhesion and remodelling of cells at the fusion plate.

In the zebrafish, the otic vesicle is a major site of expression of *gpr126*, and the defects in the *lau* mutant ear indicate a crucial function for Gpr126 in semicircular canal morphogenesis. In the mouse, initial studies using a $Gpr126^{LacZ}$ reporter did not detect expression in the ear (Waller-Evans et al., 2010). Instead, embryonic expression of murine *Gpr126* (also known as *DREG*) has been reported only in somites, heart, branchial arches, frontonasal process, kidney collecting duct and Bergmann glia of the cerebellum (Moriguchi et al., 2004; Koirala and Corfas, 2010; Pradervand et al., 2010). However, recent work by Engel and colleagues describes strong expression of *gpr126* in the mouse otic vesicle at E9.5 and E11.5 (Patra et al., 2013), suggesting possible functional conservation of this signalling pathway in otic development in mammals.

Homozygous loss of function of *Gpr126* in the mouse results in mid-gestational or perinatal lethality (depending on the allele), with a few pups surviving to 1-2 weeks of age (Waller-Evans et al., 2010; Monk et al., 2011). In surviving mutant animals, a detailed analysis

of ear structures has yet to be determined; however, no gross morphological defects in the ear have been reported. Analysis of the auditory nerve revealed a lack of peripheral myelination, with aberrant extension of central myelination by oligodendrocytes into the periphery (Monk et al., 2011), indicating that Gpr126 function in peripheral myelination is conserved between fish and mammals. It will be of interest to determine whether Gpr126 has a similarly conserved function in the development of the semicircular canal system.

Acknowledgements
We thank M. Cotterill and L. Murphy for technical assistance; G. Cooper, R. Kelsh, H. Roehl, F. van Eeden and K. Whitlock for discussion and advice; H. G. Frohnhöfer for providing fish; the Sheffield aquarium staff for expert animal care; and members of the zebrafish community for providing probes. We thank F. B. Engel for sharing information before publication, G. Corfas for advice on *Gpr126* expression in the mouse ear, and J. Jen for sequence analysis of human *GPR126*.

Funding
This work was funded by grants from the Royal National Institute for Deaf People (RNID; now Action on Hearing Loss) [S8], the Medical Research Council (MRC) [G0300196], the Wellcome Trust (084551) and the Biotechnology and Biological Sciences Research Council (BBSRC) [BB/J003050] to T.T.W., and by the EU FP6 (ZF-MODELS) [LSHG-CT-2003-503496] to M.H. The MRC Centre for Developmental and Biomedical Genetics (CDBG) zebrafish aquaria and imaging facilities were supported by the MRC [G0400100, G0700091], with additional support from the EU FP6 (ZF-MODELS) and the Wellcome Trust [GR077544AIA]. Deposited in PMC for immediate release.

Competing interests statement
The authors declare no competing financial interests.

Author contributions
F.-S.G. carried out the *gpr126* cloning, sequencing and morpholino experiments, hyaluronidase injections and phenotypic analysis. L.A. performed hyaluronidase injections, rescue experiments and gene expression analysis. S.B. carried out gene expression analysis, *sox10* mutant analysis, rescue experiments and sequence analysis, with contributions from C.J.H. A.G.S. carried out ear size measurements. K.S. and M.H. isolated the *fr24* allele; J.T. isolated and sequenced the *vu39* allele. Figures were prepared by F.-S.G., L.A., S.B., A.G.S. and T.T.W. L.A. and T.T.W. wrote the paper with contributions from F.-S.G., S.B. and J.T.

Supplementary material
Supplementary material available online at
http://dev.biologists.org/lookup/suppl/doi:10.1242/dev.098061/-/DC1

References
Abbas, L. and Whitfield, T. T. (2009). Nkcc1 (Slc12a2) is required for the regulation of endolymph volume in the otic vesicle and swim bladder volume in the zebrafish larva. *Development* **136**, 2837-2848.
Abraira, V. E., Del Rio, T., Tucker, A. F., Slonimsky, J., Keirnes, H. L. and Goodrich, L. V. (2008). Cross-repressive interactions between Lrig3 and netrin 1 shape the architecture of the inner ear. *Development* **135**, 4091-4099.
Acampora, D., Merlo, G. R., Paleari, L., Zerega, B., Postiglione, M. P., Mantero, S., Bober, E., Barbieri, O., Simeone, A. and Levi, G. (1999). Craniofacial, vestibular and bone defects in mice lacking the Distal-less-related gene Dlx5. *Development* **126**, 3795-3809.
Araç, D., Boucard, A. A., Bolliger, M. F., Nguyen, J., Soltis, S. M., Südhof, T. C. and Brunger, A. T. (2012). A novel evolutionarily conserved domain of cell-adhesion GPCRs mediates autoproteolysis. *EMBO J.* **31**, 1364-1378.
Asai, Y., Chan, D. K., Starr, C. J., Kappler, J. A., Kollmar, R. and Hudspeth, A. J. (2006). Mutation of the atrophin2 gene in the zebrafish disrupts signaling by fibroblast growth factor during development of the inner ear. *Proc. Natl. Acad. Sci. USA* **103**, 9069-9074.
Babb-Clendenon, S., Shen, Y. C., Liu, Q., Turner, K. E., Mills, M. S., Cook, G. W., Miller, C. A., Gattone, V. H., 2nd, Barald, K. F. and Marrs, J. A. (2006). Cadherin-2 participates in the morphogenesis of the zebrafish inner ear. *J. Cell Sci.* **119**, 5169-5177.
Bahary, N., Davidson, A., Ransom, D., Shepard, J., Stern, H., Trede, N., Zhou, Y., Barut, B. and Zon, L. I. (2004). The Zon laboratory guide to positional cloning in zebrafish. *Methods Cell Biol.* **77**, 305-329.
Bakkers, J., Kramer, C., Pothof, J., Quaedvlieg, N. E., Spaink, H. P. and Hammerschmidt, M. (2004). Has2 is required upstream of Rac1 to govern dorsal migration of lateral cells during zebrafish gastrulation. *Development* **131**, 525-537.
Bissonnette, J. P. and Fekete, D. M. (1996). Standard atlas of the gross anatomy of the developing inner ear of the chicken. *J. Comp. Neurol.* **368**, 620-630.
Bjarnadóttir, T. K., Fredriksson, R., Höglund, P. J., Gloriam, D. E., Lagerström, M. C. and Schiöth, H. B. (2004). The human and mouse repertoire of the adhesion family of G-protein-coupled receptors. *Genomics* **84**, 23-33.
Bjarnadóttir, T. K., Fredriksson, R. and Schiöth, H. B. (2007). The adhesion GPCRs: a unique family of G protein-coupled receptors with important roles in both central and peripheral tissues. *Cell. Mol. Life Sci.* **64**, 2104-2119.
Blasiole, B., Kabbani, N., Boehmler, W., Thisse, B., Thisse, C., Canfield, V. and Levenson, R. (2005). Neuronal calcium sensor-1 gene ncs-1a is essential for semicircular canal formation in zebrafish inner ear. *J. Neurobiol.* **64**, 285-297.
Blasiole, B., Canfield, V. A., Vollrath, M. A., Huss, D., Mohideen, M. A., Dickman, J. D., Cheng, K. C., Fekete, D. M. and Levenson, R. (2006). Separate Na,K-ATPase genes are required for otolith formation and semicircular canal development in zebrafish. *Dev. Biol.* **294**, 148-160.
Bok, J., Chang, W. and Wu, D. K. (2007). Patterning and morphogenesis of the vertebrate inner ear. *Int. J. Dev. Biol.* **51**, 521-533.
Brösamle, C. and Halpern, M. E. (2002). Characterization of myelination in the developing zebrafish. *Glia* **39**, 47-57.
Busch-Nentwich, E., Söllner, C., Roehl, H. and Nicolson, T. (2004). The deafness gene dfna5 is crucial for ugdh expression and HA production in the developing ear in zebrafish. *Development* **131**, 943-951.
Cantos, R., Cole, L. K., Acampora, D., Simeone, A. and Wu, D. K. (2000). Patterning of the mammalian cochlea. *Proc. Natl. Acad. Sci. USA* **97**, 11707-11713.
Carney, T. J., Feitosa, N. M., Sonntag, C., Slanchev, K., Kluger, J., Kiyozumi, D., Gebauer, J. M., Coffin Talbot, J., Kimmel, C. B., Sekiguchi, K. et al. (2010). Genetic analysis of fin development in zebrafish identifies furin and hemicentin1 as potential novel fraser syndrome disease genes. *PLoS Genet.* **6**, e1000907.
Cecconi, F., Roth, K. A., Dolgov, O., Munarriz, E., Anokhin, K., Gruss, P. and Salminen, M. (2004). Apaf1-dependent programmed cell death is required for inner ear morphogenesis and growth. *Development* **131**, 2125-2135.
Chang, W., Brigande, J. V., Fekete, D. M. and Wu, D. K. (2004). The development of semicircular canals in the inner ear: role of FGFs in sensory cristae. *Development* **131**, 4201-4211.
Chang, W., Lin, Z., Kulessa, H., Hebert, J., Hogan, B. L. and Wu, D. K. (2008). Bmp4 is essential for the formation of the vestibular apparatus that detects angular head movements. *PLoS Genet.* **4**, e1000050.
Chen, W. Y. and Abatangelo, G. (1999). Functions of hyaluronan in wound repair. *Wound Repair Regen.* **7**, 79-89.
Chiang, E. F.-L., Pai, C.-I., Wyatt, M., Yan, Y.-L., Postlethwait, J. and Chung, B.-C. (2001). Two sox9 genes on duplicated zebrafish chromosomes: expression of similar transcription activators in distinct sites. *Dev. Biol.* **231**, 149-163.
Cruz, S., Shiao, J. C., Liao, B. K., Huang, C. J. and Hwang, P. P. (2009). Plasma membrane calcium ATPase required for semicircular canal formation and otolith growth in the zebrafish inner ear. *J. Exp. Biol.* **212**, 639-647.
Deng, M., Pan, L., Xie, X. and Gan, L. (2010). Requirement for Lmo4 in the vestibular morphogenesis of mouse inner ear. *Dev. Biol.* **338**, 38-49.
Dutton, K. A., Pauliny, A., Lopes, S. S., Elworthy, S., Carney, T. J., Rauch, J., Geisler, R., Haffter, P. and Kelsh, R. N. (2001). Zebrafish colourless encodes sox10 and specifies non-ectomesenchymal neural crest fates. *Development* **128**, 4113-4125.
Dutton, K., Abbas, L., Spencer, J., Brannon, C., Mowbray, C., Nikaido, M., Kelsh, R. N. and Whitfield, T. T. (2009). A zebrafish model for Waardenburg syndrome type IV reveals diverse roles for Sox10 in the otic vesicle. *Dis. Model. Mech.* **2**, 68-83.
Elks, M. L. and Manganiello, V. C. (1985). A role for soluble cAMP phosphodiesterases in differentiation of 3T3-L1 adipocytes. *J. Cell. Physiol.* **124**, 191-198.
Enomoto, H., Nelson, C. M., Somerville, R. P., Mielke, K., Dixon, L. J., Powell, K. and Apte, S. S. (2010). Cooperation of two ADAMTS metalloproteases in closure of the mouse palate identifies a requirement for versican proteolysis in regulating palatal mesenchyme proliferation. *Development* **137**, 4029-4038.
Everett, L. A., Belyantseva, I. A., Noben-Trauth, K., Cantos, R., Chen, A., Thakkar, S. I., Hoogstraten-Miller, S. L., Kachar, B., Wu, D. K. and Green, E. D. (2001). Targeted disruption of mouse Pds provides insight about the inner-ear defects encountered in Pendred syndrome. *Hum. Mol. Genet.* **10**, 153-161.
Fekete, D. M., Homburger, S. A., Waring, M. T., Riedl, A. E. and Garcia, L. F. (1997). Involvement of programmed cell death in morphogenesis of the vertebrate inner ear. *Development* **124**, 2451-2461.
Fritzsch, B., Signore, M. and Simeone, A. (2001). Otx1 null mutant mice show partial segregation of sensory epithelia comparable to lamprey ears. *Dev. Genes Evol.* **211**, 388-396.

Glenn, T. D. and Talbot, W. S. (2013). Analysis of Gpr126 function defines distinct mechanisms controlling the initiation and maturation of myelin. *Development* **140**, 3167-3175.
Haddon, C. M. and Lewis, J. H. (1991). Hyaluronan as a propellant for epithelial movement: the development of semicircular canals in the inner ear of Xenopus. *Development* **112**, 541-550.
Haddon, C. and Lewis, J. (1996). Early ear development in the embryo of the zebrafish, Danio rerio. *J. Comp. Neurol.* **365**, 113-128.
Hadrys, T., Braun, T., Rinkwitz-Brandt, S., Arnold, H.-H. and Bober, E. (1998). Nkx5-1 controls semicircular canal formation in the mouse inner ear. *Development* **125**, 33-39.
Hammerschmidt, M., Serbedzija, G. N. and McMahon, A. P. (1996). Genetic analysis of dorsoventral pattern formation in the zebrafish: requirement of a BMP-like ventralizing activity and its dorsal repressor. *Genes Dev.* **10**, 2452-2461.
Hammond, K. L. and Whitfield, T. T. (2006). The developing lamprey ear closely resembles the zebrafish otic vesicle: otx1 expression can account for all major patterning differences. *Development* **133**, 1347-1357.
Hammond, K. L., van Eeden, F. J. and Whitfield, T. T. (2010). Repression of Hedgehog signalling is required for the acquisition of dorsolateral cell fates in the zebrafish otic vesicle. *Development* **137**, 1361-1371.
Han, Y., Mu, Y., Li, X., Xu, P., Tong, J., Liu, Z., Ma, T., Zeng, G., Yang, S., Du, J. et al. (2011). Grhl2 deficiency impairs otic development and hearing ability in a zebrafish model of the progressive dominant hearing loss DFNA28. *Hum. Mol. Genet.* **20**, 3213-3226.
Hatano, S., Kimata, K., Hiraiwa, N., Kusakabe, M., Isogai, Z., Adachi, E., Shinomura, T. and Watanabe, H. (2012). Versican/PG-M is essential for ventricular septal formation subsequent to cardiac atrioventricular cushion development. *Glycobiology* **22**, 1268-1277.
Hulander, M., Kiernan, A. E., Blomqvist, S. R., Carlsson, P., Samuelsson, E. J., Johansson, B. R., Steel, K. P. and Enerbäck, S. (2003). Lack of pendrin expression leads to deafness and expansion of the endolymphatic compartment in inner ears of Foxi1 null mutant mice. *Development* **130**, 2013-2025.
Jalink, K. and Moolenaar, W. H. (2010). G protein-coupled receptors: the inside story. *Bioessays* **32**, 13-16.
Kang, J. S., Oohashi, T., Kawakami, Y., Bekku, Y., Izpisúa Belmonte, J. C. and Ninomiya, Y. (2004). Characterization of dermacan, a novel zebrafish lectican gene, expressed in dermal bones. *Mech. Dev.* **121**, 301-312.
Kang, J. S., Kawakami, Y., Bekku, Y., Ninomiya, Y., Izpisúa Belmonte, J. C. and Oohashi, T. (2008). Molecular cloning and developmental expression of a hyaluronan and proteoglycan link protein gene, crtl1/hapln1, in zebrafish. *Zoolog. Sci.* **25**, 912-918.
Kelsh, R. N., Dutton, K., Medlin, J. and Eisen, J. S. (2000). Expression of zebrafish fkd6 in neural crest-derived glia. *Mech. Dev.* **93**, 161-164.
Kobayashi, Y., Nakamura, H. and Funahashi, J.-I. (2008). Epithelial-mesenchymal transition as a possible mechanism of semicircular canal morphogenesis in chick inner ear. *Tohoku J. Exp. Med.* **215**, 207-217.
Koirala, S. and Corfas, G. (2010). Identification of novel glial genes by single-cell transcriptional profiling of Bergmann glial cells from mouse cerebellum. *PLoS ONE* **5**, e9198.
Kwakkenbos, M. J., Pouwels, W., Matmati, M., Stacey, M., Lin, H. H., Gordon, S., van Lier, R. A. and Hamann, J. (2005). Expression of the largest CD97 and EMR2 isoforms on leukocytes facilitates a specific interaction with chondroitin sulfate on B cells. *J. Leukoc. Biol.* **77**, 112-119.
Lang, H., Bever, M. M. and Fekete, D. M. (2000). Cell proliferation and cell death in the developing chick inner ear: spatial and temporal patterns. *J. Comp. Neurol.* **417**, 205-220.
Lang, F., Vallon, V., Knipper, M. and Wangemann, P. (2007). Functional significance of channels and transporters expressed in the inner ear and kidney. *Am. J. Physiol.* **293**, C1187-C1208.
Li, Y., Laue, K., Temtamy, S., Aglan, M., Kotan, L. D., Yigit, G., Canan, H., Pawlik, B., Nürnberg, G., Wakeling, E. L. et al. (2010). Temtamy preaxial brachydactyly syndrome is caused by loss-of-function mutations in chondroitin synthase 1, a potential target of BMP signaling. *Am. J. Hum. Genet.* **87**, 757-767.
Lin, Z., Cantos, R., Patente, M. and Wu, D. K. (2005). Gbx2 is required for the morphogenesis of the mouse inner ear: a downstream candidate of hindbrain signaling. *Development* **132**, 2309-2318.
Lister, J. A., Robertson, C. P., Lepage, T., Johnson, S. L. and Raible, D. W. (1999). nacre encodes a zebrafish microphthalmia-related protein that regulates neural-crest-derived pigment cell fate. *Development* **126**, 3757-3767.
Martin, P. and Swanson, G. J. (1993). Descriptive and experimental analysis of the epithelial remodellings that control semicircular canal formation in the developing mouse inner ear. *Dev. Biol.* **159**, 549-558.
Megerian, C. A., Semaan, M. T., Aftab, S., Kisley, L. B., Zheng, Q. Y., Pawlowski, K. S., Wright, C. G. and Alagramam, K. N. (2008). A mouse model with postnatal endolymphatic hydrops and hearing loss. *Hear. Res.* **237**, 90-105.
Merlo, G. R., Paleari, L., Mantero, S., Zerega, B., Adamska, M., Rinkwitz, S., Bober, E. and Levi, G. (2002). The Dlx5 homeobox gene is essential for vestibular morphogenesis in the mouse embryo through a BMP4-mediated pathway. *Dev. Biol.* **248**, 157-169.
Michelmore, R. W., Paran, I. and Kesseli, R. V. (1991). Identification of markers linked to disease-resistance genes by bulked segregant analysis: a rapid method to detect markers in specific genomic regions by using segregating populations. *Proc. Natl. Acad. Sci. USA* **88**, 9828-9832.
Milhaud, P. G., Pondugula, S. R., Lee, J. H., Herzog, M., Lehouelleur, J., Wangemann, P., Sans, A. and Marcus, D. C. (2002). Chloride secretion by semicircular canal duct epithelium is stimulated via beta 2-adrenergic receptors. *Am. J. Physiol.* **283**, C1752-C1760.
Monk, K. R., Naylor, S. G., Glenn, T. D., Mercurio, S., Perlin, J. R., Dominguez, C., Moens, C. B. and Talbot, W. S. (2009). A G protein-coupled receptor is essential for Schwann cells to initiate myelination. *Science* **325**, 1402-1405.
Monk, K. R., Oshima, K., Jörs, S., Heller, S. and Talbot, W. S. (2011). Gpr126 is essential for peripheral nerve development and myelination in mammals. *Development* **138**, 2673-2680.
Moriguchi, T., Haraguchi, K., Ueda, N., Okada, M., Furuya, T. and Akiyama, T. (2004). DREG, a developmentally regulated G protein-coupled receptor containing two conserved proteolytic cleavage sites. *Genes Cells* **9**, 549-560.
Morsli, H., Tuorto, F., Choo, D., Postiglione, M. P., Simeone, A. and Wu, D. K. (1999). Otx1 and Otx2 activities are required for the normal development of the mouse inner ear. *Development* **126**, 2335-2343.
Neuhauss, S. C. F., Solnica-Krezel, L., Schier, A. F., Zwartkruis, F., Stemple, D. L., Malicki, J., Abdelilah, S., Stainier, D. Y. R. and Driever, W. (1996). Mutations affecting craniofacial development in zebrafish. *Development* **123**, 357-367.
Noda, T., Oki, S., Kitajima, K., Harada, T., Komune, S. and Meno, C. (2012). Restriction of Wnt signaling in the dorsal otocyst determines semicircular canal formation in the mouse embryo. *Dev. Biol.* **362**, 83-93.
Nüsslein-Volhard, C. and Dahm, R. (2002). *Zebrafish: A Practical Approach*. Oxford: Oxford University Press.
Odenthal, J. and Nüsslein-Volhard, C. (1998). fork head domain genes in zebrafish. *Dev. Genes Evol.* **208**, 245-258.
Oka, Y., Saraiva, L. R., Kwan, Y. Y. and Korsching, S. I. (2009). The fifth class of Galpha proteins. *Proc. Natl. Acad. Sci. USA* **106**, 1484-1489.
Patra, C., van Amerongen, M. J., Ghosh, S., Ricciardi, F., Sajjad, A., Novoyatleva, T., Mogha, A., Monk, K. R., Mühlfeld, C. and Engel, F. B. (2013). Organ-specific function of adhesion G protein-coupled receptor GPR126 is domain dependent. *Proc. Natl. Acad. Sci. USA* (in press).
Pfeffer, P. L., Gerster, T., Lun, K., Brand, M. and Busslinger, M. (1998). Characterization of three novel members of the zebrafish Pax2/5/8 family: dependency of Pax5 and Pax8 expression on the Pax2.1 (noi) function. *Development* **125**, 3063-3074.
Piotrowski, T., Ahn, D.-G., Schilling, T. F., Nair, S., Ruvinsky, I., Geisler, R., Rauch, G.-J., Haffter, P., Zon, L. I., Zhou, Y. et al. (2003). The zebrafish van gogh mutation disrupts tbx1, which is involved in the DiGeorge deletion syndrome in humans. *Development* **130**, 5043-5052.
Pittlik, S., Domingues, S., Meyer, A. and Begemann, G. (2008). Expression of zebrafish aldh1a3 (raldh3) and absence of aldh1a1 in teleosts. *Gene Expr. Patterns* **8**, 141-147.
Pogoda, H. M., Sternheim, N., Lyons, D. A., Diamond, B., Hawkins, T. A., Woods, I. G., Bhatt, D. H., Franzini-Armstrong, C., Dominguez, C., Arana, N. et al. (2006). A genetic screen identifies genes essential for development of myelinated axons in zebrafish. *Dev. Biol.* **298**, 118-131.
Pondugula, S. R., Kampalli, S. B., Wu, T., De Lisle, R. C., Raveendran, N. N., Harbidge, D. G. and Marcus, D. C. (2013). cAMP-stimulated Cl- secretion is increased by glucocorticoids and inhibited by bumetanide in semicircular canal duct epithelium. *BMC Physiol.* **13**, 6.
Pradervand, S., Zuber Mercier, A., Centeno, G., Bonny, O. and Firsov, D. (2010). A comprehensive analysis of gene expression profiles in distal parts of the mouse renal tubule. *Pflugers Archiv.* **460**, 925-952.
Rakowiecki, S. and Epstein, D. J. (2013). Divergent roles for Wnt/β-catenin signaling in epithelial maintenance and breakdown during semicircular canal formation. *Development* **140**, 1730-1739.
Reifers, F., Böhli, H., Walsh, E. C., Crossley, P. H., Stainier, D. Y. R. and Brand, M. (1998). Fgf8 is mutated in zebrafish acerebellar (ace) mutants and is required for maintenance of midbrain-hindbrain boundary development and somitogenesis. *Development* **125**, 2381-2395.
Ricciardelli, C., Sakko, A. J., Ween, M. P., Russell, D. L. and Horsfall, D. J. (2009). The biological role and regulation of versican levels in cancer. *Cancer Metastasis Rev.* **28**, 233-245.
Sahly, I., Andermann, P. and Petit, C. (1999). The zebrafish eya1 gene and its expression pattern during embryogenesis. *Dev. Genes Evol.* **209**, 399-410.
Salminen, M., Meyer, B. I., Bober, E. and Gruss, P. (2000). Netrin 1 is required for semicircular canal formation in the mouse inner ear. *Development* **127**, 13-22.
Schultz, G., Hardman, J. G., Schultz, K., Davis, J. W. and Sutherland, E. W. (1973). A new enzymatic assay for guanosine 3′:5′-cyclic monophosphate and

its application to the ductus deferens of the rat. *Proc. Natl. Acad. Sci. USA* **70**, 1721-1725.
Seamon, K. and Daly, J. W. (1981). Activation of adenylate cyclase by the diterpene forskolin does not require the guanine nucleotide regulatory protein. *J. Biol. Chem.* **256**, 9799-9801.
Shawi, M. and Serluca, F. C. (2008). Identification of a BMP7 homolog in zebrafish expressed in developing organ systems. *Gene Expr. Patterns* **8**, 369-375.
Solomon, K. S., Kudoh, T., Dawid, I. B. and Fritz, A. (2003). Zebrafish foxi1 mediates otic placode formation and jaw development. *Development* **130**, 929-940.
Stacey, M., Chang, G. W., Davies, J. Q., Kwakkenbos, M. J., Sanderson, R. D., Hamann, J., Gordon, S. and Lin, H. H. (2003). The epidermal growth factor-like domains of the human EMR2 receptor mediate cell attachment through chondroitin sulfate glycosaminoglycans. *Blood* **102**, 2916-2924.
Sunose, H., Liu, J. and Marcus, D. C. (1997a). cAMP increases K+ secretion via activation of apical IsK/KvLQT1 channels in strial marginal cells. *Hear. Res.* **114**, 107-116.
Sunose, H., Liu, J., Shen, Z. and Marcus, D. C. (1997b). cAMP increases apical IsK channel current and K+ secretion in vestibular dark cells. *J. Membr. Biol.* **156**, 25-35.
Thisse, B. and Thisse, C. (2004). Fast release clones: a high throughput expression analysis. *ZFIN Direct Data Submission* (http://zfin.org).
Van Laer, L., Pfister, M., Thys, S., Vrijens, K., Mueller, M., Umans, L., Serneels, L., Van Nassauw, L., Kooy, F., Smith, R. J. et al. (2005). Mice lacking Dfna5 show a diverging number of cochlear fourth row outer hair cells. *Neurobiol. Dis.* **19**, 386-399.
Waller-Evans, H., Prömel, S., Langenhan, T., Dixon, J., Zahn, D., Colledge, W. H., Doran, J., Carlton, M. B., Davies, B., Aparicio, S. A. et al. (2010). The orphan adhesion-GPCR GPR126 is required for embryonic development in the mouse. *PLoS ONE* **5**, e14047.
Wang, W., Chan, E. K., Baron, S., Van de Water, T. and Lufkin, T. (2001). Hmx2 homeobox gene control of murine vestibular morphogenesis. *Development* **128**, 5017-5029.
Wang, W., Grimmer, J. F., Van De Water, T. R. and Lufkin, T. L. (2004). Hmx2 and Hmx3 homeobox genes direct development of the murine inner ear and hypothalamus and can be functionally replaced by Drosophila Hmx. *Dev. Cell* **7**, 439-453.
Waterman, R. E. and Bell, D. H. (1984). Epithelial fusion during early semicircular canal formation in the embryonic zebrafish, Brachydanio rerio. *Anat. Rec.* **210**, 101-114.
Westerfield, M. (2000). *The Zebrafish Book. A Guide for the Laboratory Use of Zebrafish (Danio rerio)*. Eugene, OR: University of Oregon Press.
Whitfield, T. T., Granato, M., van Eeden, F. J. M., Schach, U., Brand, M., Furutani-Seiki, M., Haffter, P., Hammerschmidt, M., Heisenberg, C.-P., Jiang, Y.-J. et al. (1996). Mutations affecting development of the zebrafish inner ear and lateral line. *Development* **123**, 241-254.
Wight, T. N. (2002). Versican: a versatile extracellular matrix proteoglycan in cell biology. *Curr. Opin. Cell Biol.* **14**, 617-623.
Yona, S., Lin, H. H., Siu, W. O., Gordon, S. and Stacey, M. (2008). Adhesion-GPCRs: emerging roles for novel receptors. *Trends Biochem. Sci.* **33**, 491-500.

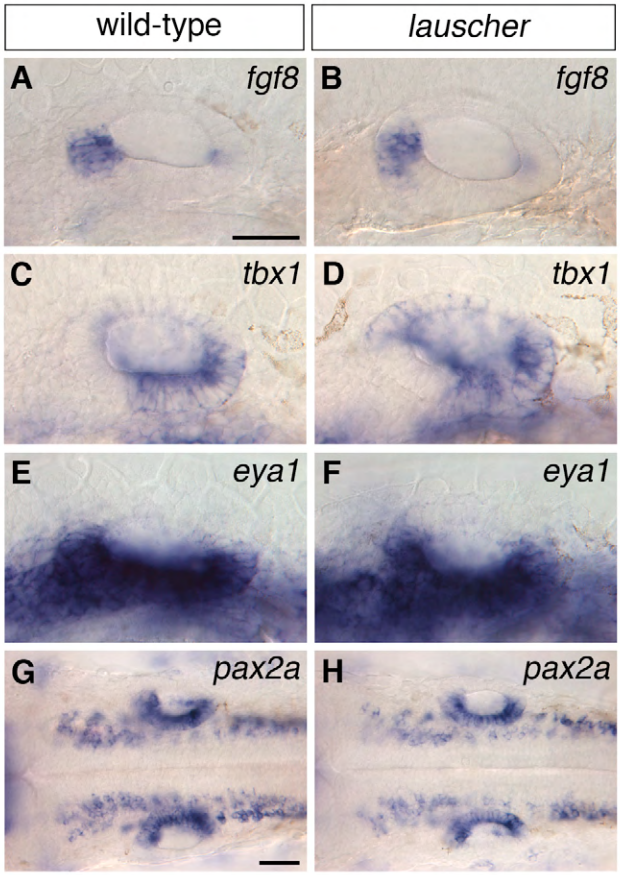

Figure S1. Expression of early otic patterning markers is normal in *lauscher* mutants. (A-J) Expression of early patterning markers in the otic vesicle is indistinguishable between wild-types and homozygous *lau*^{tb233c} mutants. Normal expression is seen for *fgf8a* (*fgf8*) anteriorly (A,B), *tbx1* posteriorly (C,D), *eya1* ventrally (E,F) and *pax2a* medially (G,H) at 27 hpf. Scale bars: A, 50µm (applies to B-F); G, 50µm (applies to H).

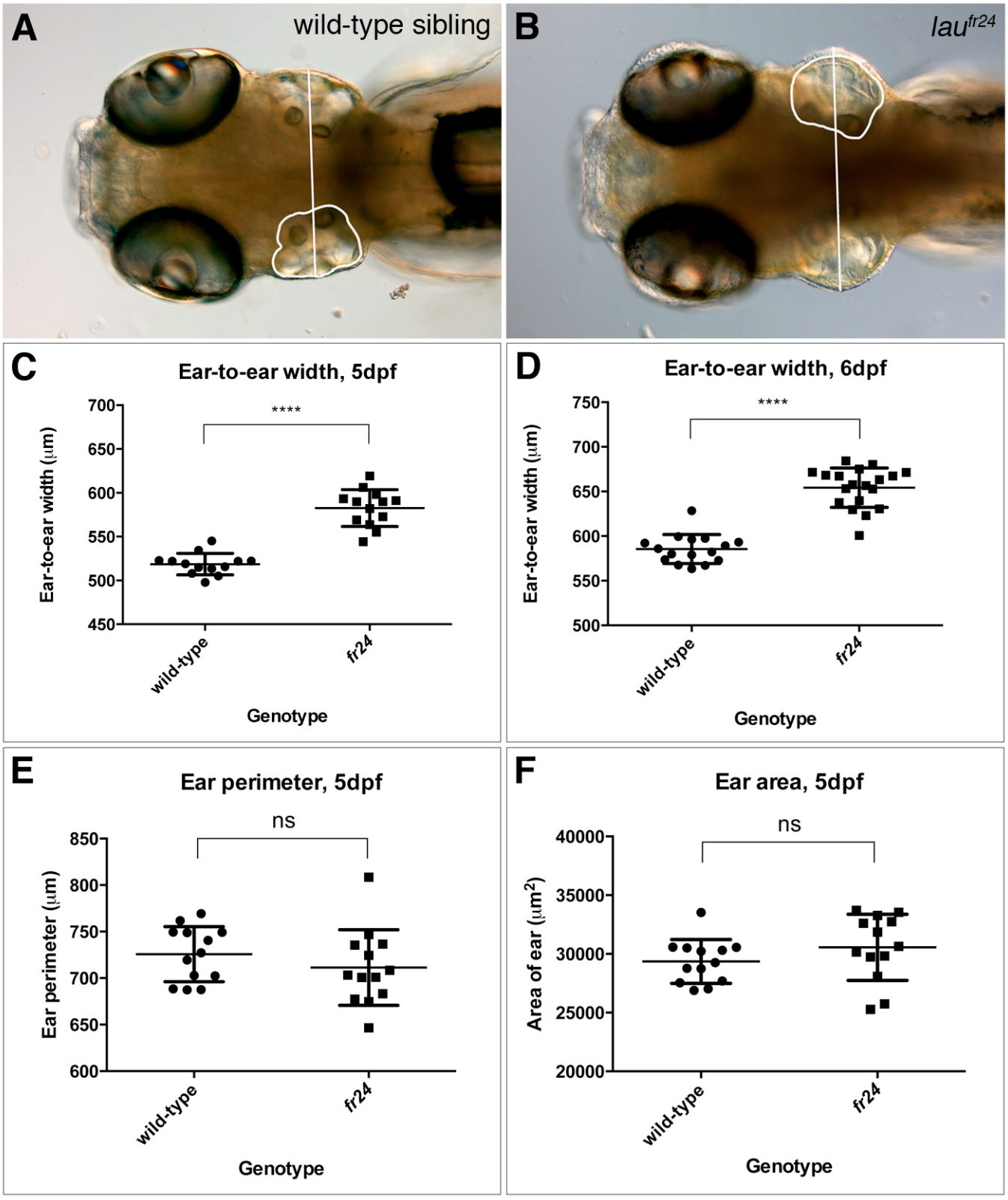

Figure S2. Quantitation of the *lauscher* swollen ear phenotype. (A,B) Sample micrographs showing dorsal views of live wild-type sibling (A) and *lau*^{fr24} mutant (B) embryos at 5 dpf. Measurements were taken of ear-to-ear width (straight white line) and ear perimeter (white line outlining ear) using CELLB software (Olympus). Embryos were treated with 1-phenyl 2-thiourea (PTU) to suppress development of pigmentation. Embryos were photographed at a focal plane that highlighted the largest visible dimensions for the parameters shown, and the ear chosen for measurement in each micrograph was the one with the most clearly visible outline. Ear cross-sectional area was calculated from the perimeter drawn, using CELLB software (Olympus). **(C-F)** Quantitation of ear-to-ear width (C,D), ear perimeter (E) and ear area (F); data were plotted using Prism 6 (GraphPad software). $N \geq 13$ for each data set. Error bars indicate standard deviation; ****$P<0.0001$ (unpaired, two-tailed *t*-test); ns, not significant.

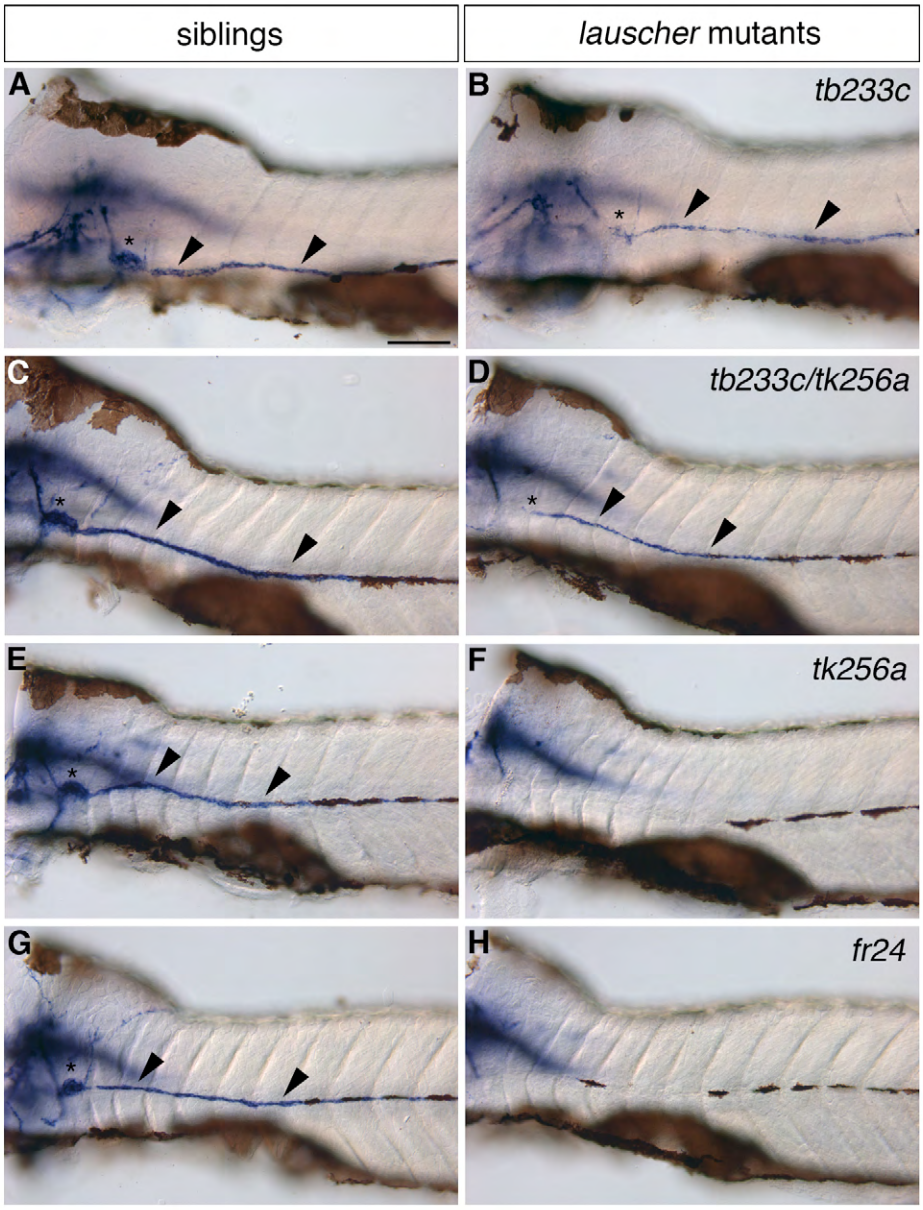

Figure S3. Expression of the *myelin basic protein* gene (*mbpa*) is lost or reduced in the posterior lateral line ganglion and nerve in *lauscher* mutants. (A-H) Whole mount in situ hybridisation at 5 days post fertilisation shows a reduction in *mbpa* (*mbp*) expression in Schwann cells of the posterior lateral line ganglion (asterisks) and nerve (arrowheads) in the hypomorphic *tb233c* homozygotes (B) and *tb233c/tk256a* transheterozygotes (D); expression is lost in *tk256a* (F) and *fr24* homozygotes (H). Lateral views. Scale bar: 100µm throughout.

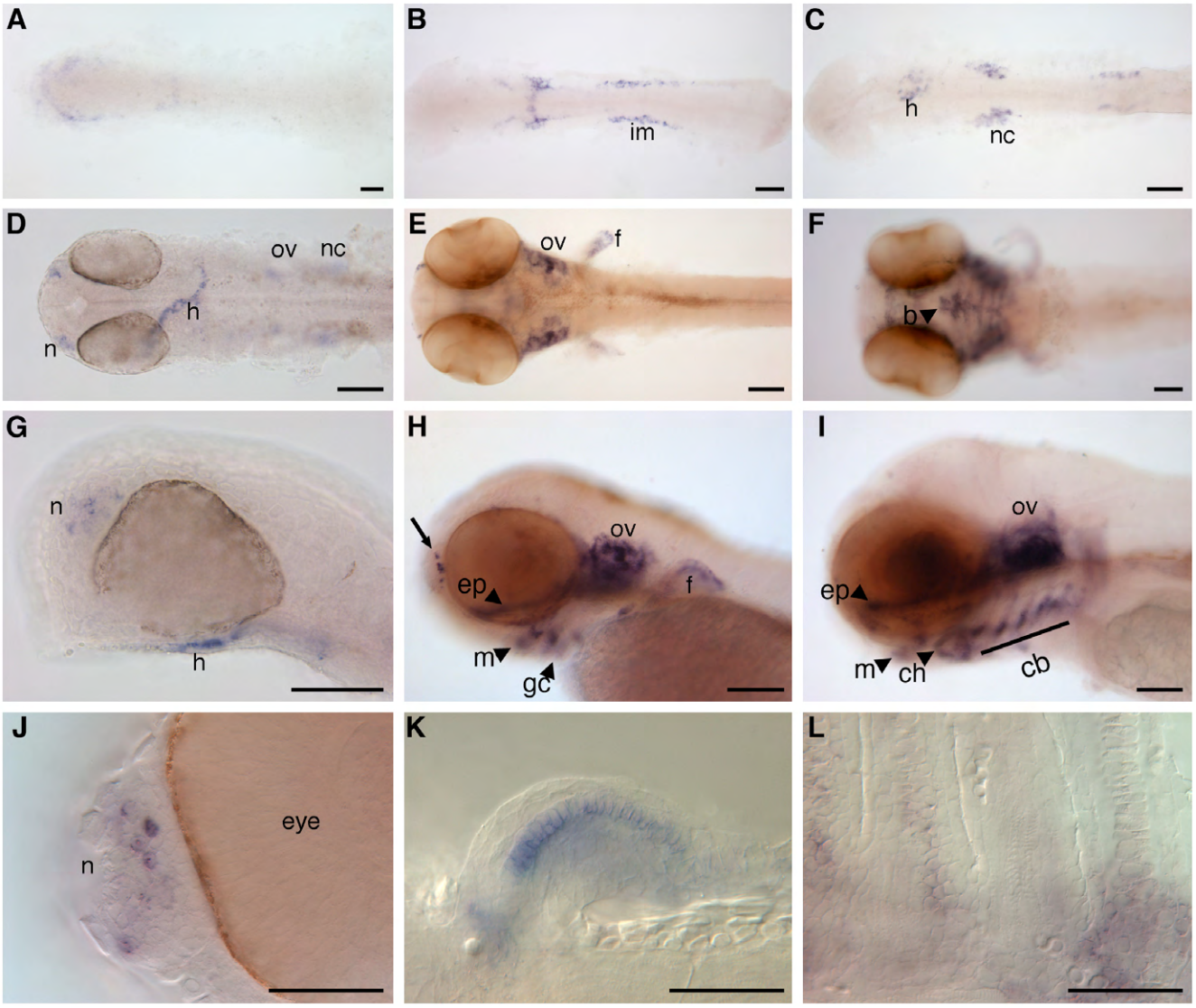

Figure S4. Expression of *gpr126* mRNA at other sites during zebrafish development. (A-C) Flat mounted embryos at 5 somites (A), 14 somites (B) and 23 somites (C). Patchy expression of *gpr126* is seen the anterior of the embryo and also in presumed neural crest (A). At 14 somites, weak expression is seen in the presumed developing heart fields, neural crest and intermediate mesoderm (im; precursor of the pronephric ducts) (B). At 23 somites, expression increases in the migrating heart tube (h) and neural crest (nc) (C). **(D,G,J)** Expression at 24 hpf in dorsal (D), lateral (G) and detailed (J) view, showing expression in the post-otic neural crest (nc), heart tube (h) and olfactory epithelium (nose, n). J shows staining of individual cells within the olfactory epithelium. **(E,H,K)** 48 hpf embryos in dorsal (E), lateral (H) and detailed (K) view. Expression continues in the nose (arrow, H), but is reduced in the heart and lost in the post-otic ganglia. New expression is seen in the ear (ov), pectoral fin (f) and tail fin (not shown), and chondrocytes of the head (arrowheads). K shows expression of *gpr126* in the chondrocytes of the pectoral fin. **(F,I,L)** 72 hpf embryos in dorsal (F), lateral (I) and detailed (L) view. Expression continues in the ear, nose, fins and head chondrocytes (arrowheads and line). Detailed view of *gpr12* expression in posterior ceratobranchials is shown in L. By 96 hpf, expression of *gpr126* remains primarily in the ear (not shown). Abbreviations: b, basihyal; cb, ceratobranchials; ep, ethmoid plate; ch, ceratohyal; f, pectoral fin; gc, gill cartilages; h, heart; im, intermediate mesoderm; m, Meckel's cartilage, n, nose (olfactory epithelium); nc, neural crest; ov, otic vesicle. Scale bars: A-I, 100 µm; J-L, 50 µm.

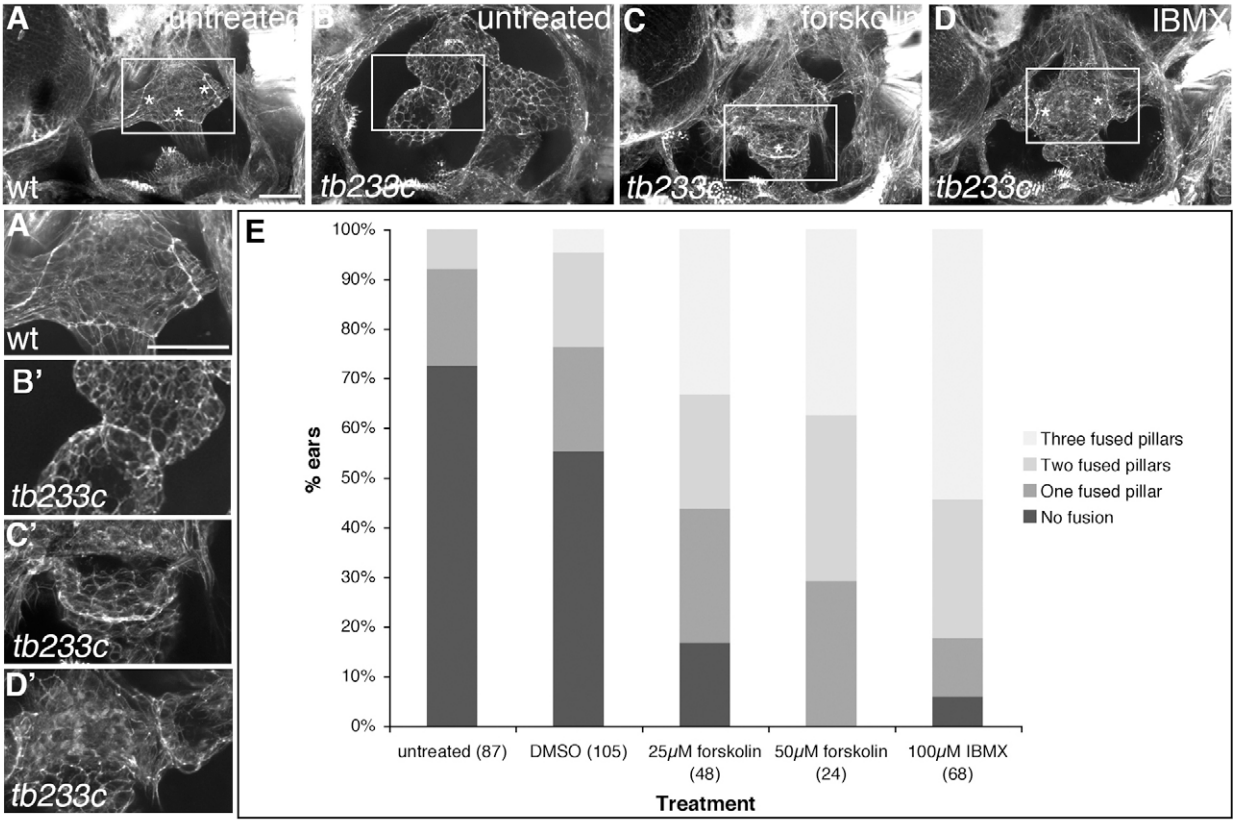

Figure S5. Treatment with cAMP agonists can rescue fusion plate formation in *lauscher* mutant embryos. (A-D') Confocal images of ears stained with FITC-phalloidin (marking F actin) to show morphology of the canal projections and pillars. Concentrations of actin mark the fusion plates (shown at higher magnification in A'-D'). (A, A') Wild-type ear. Three fusion plates are clearly visible (asterisks). (B,B') Untreated ear from a homozygous *tb233c* mutant. Canal tissue is very disorganised. Although projections are touching in this ear, analysis of the z-stack indicated that this was not a true fusion plate. (C-D') Treatment of homozygous *tb233c* embryos with either 50μM forskolin or 100μM IBMX can restore pillar formation. Fusion plates appear relatively normal. **(E)** Quantitation of the number of fusion plates present. Data were analysed with a 4×3 chi-square contingency table (DMSO, forskolin) or a 4×2 chi-square contingency table (DMSO, IBMX); $P<0.001$ for both drugs. *N* numbers are shown in parentheses. Lateral views. Scale bars: A-D 50μm; A'-D' 50μm.

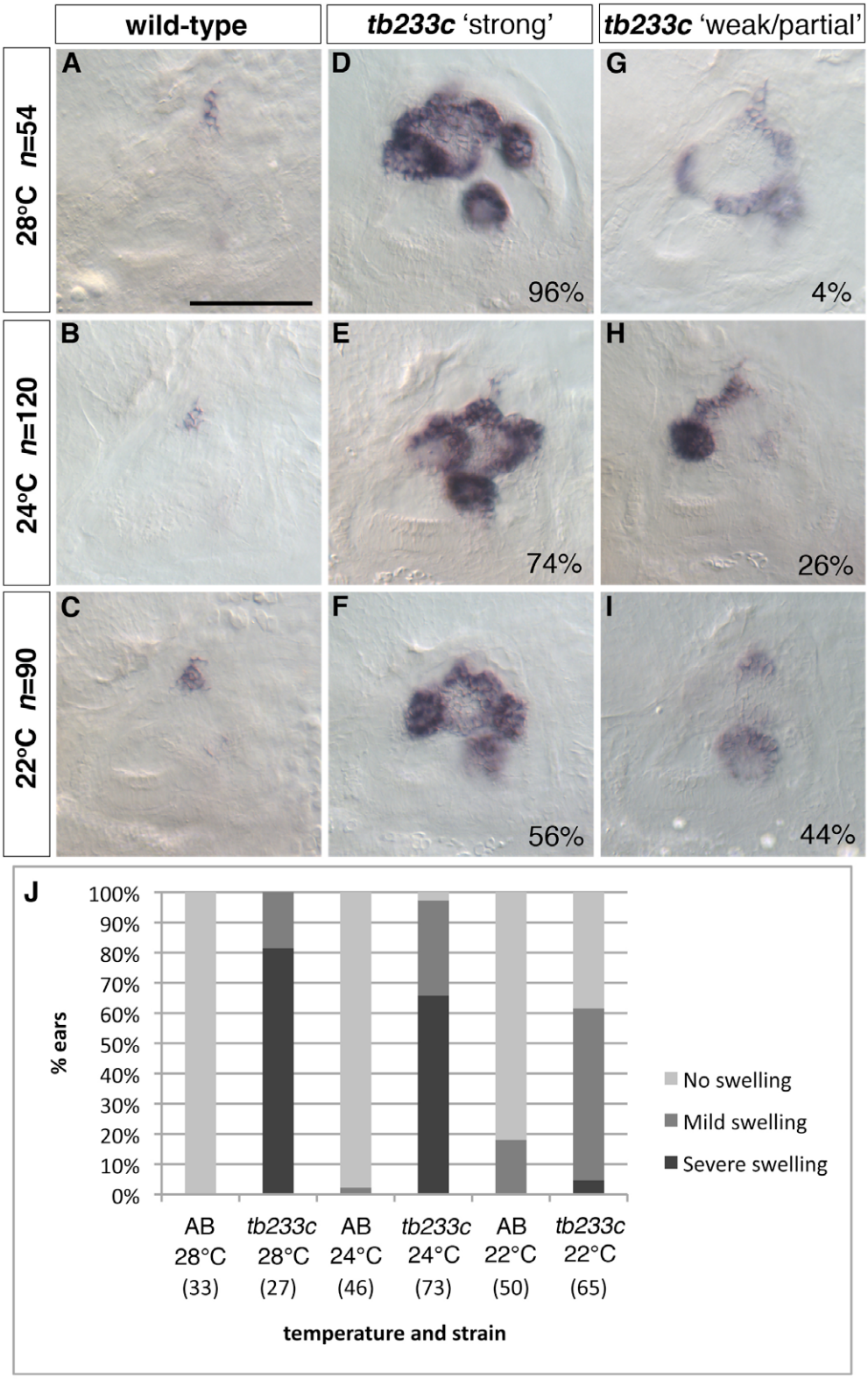

Figure S6. Incubation of *lau*^{tb233c} mutants at a lower temperature throughout the fusion period has a rescuing effect on otic *versican* expression and projection fusion. (**A-I**) Expression of *vcanb* in 4dpf wild-type (A-C), and *tb233c* (B-I) embryos, incubated at 28˚C (A,D,G), 24˚C (B,E,H) and 22˚C (C,F,I). Embryos were initially grown for 24 hours at 28˚C. In wild-type embryos, *vcanb* expression is down-regulated in the fused pillars; staining only remains in the dorsolateral septum (DLS) (A-C). Mutant embryos retain strong *vcanb* expression in the unfused projections (D-F). Some mutant embryos show weaker expression (G) or partial expression where there are fused and unfused pillars in the same ear (H,I). The proportion of embryos showing decreased *vcanb* expression and rescue of fusion increases with a decrease in temperature. Percentages for each phenotypic class are shown on the panels; *N* numbers (number of mutant ears analysed) are shown in the boxes at the left. (**J**) Graphical representation of ear swelling data for wild-type and mutant embryos grown at different temperatures. The rescue of fusion in one or more pillars results in a decrease of swelling in the ear. Embryos grown at lower temperatures have reduced swelling in the ear. *N* numbers (number of mutant ears analysed) are shown in parentheses.

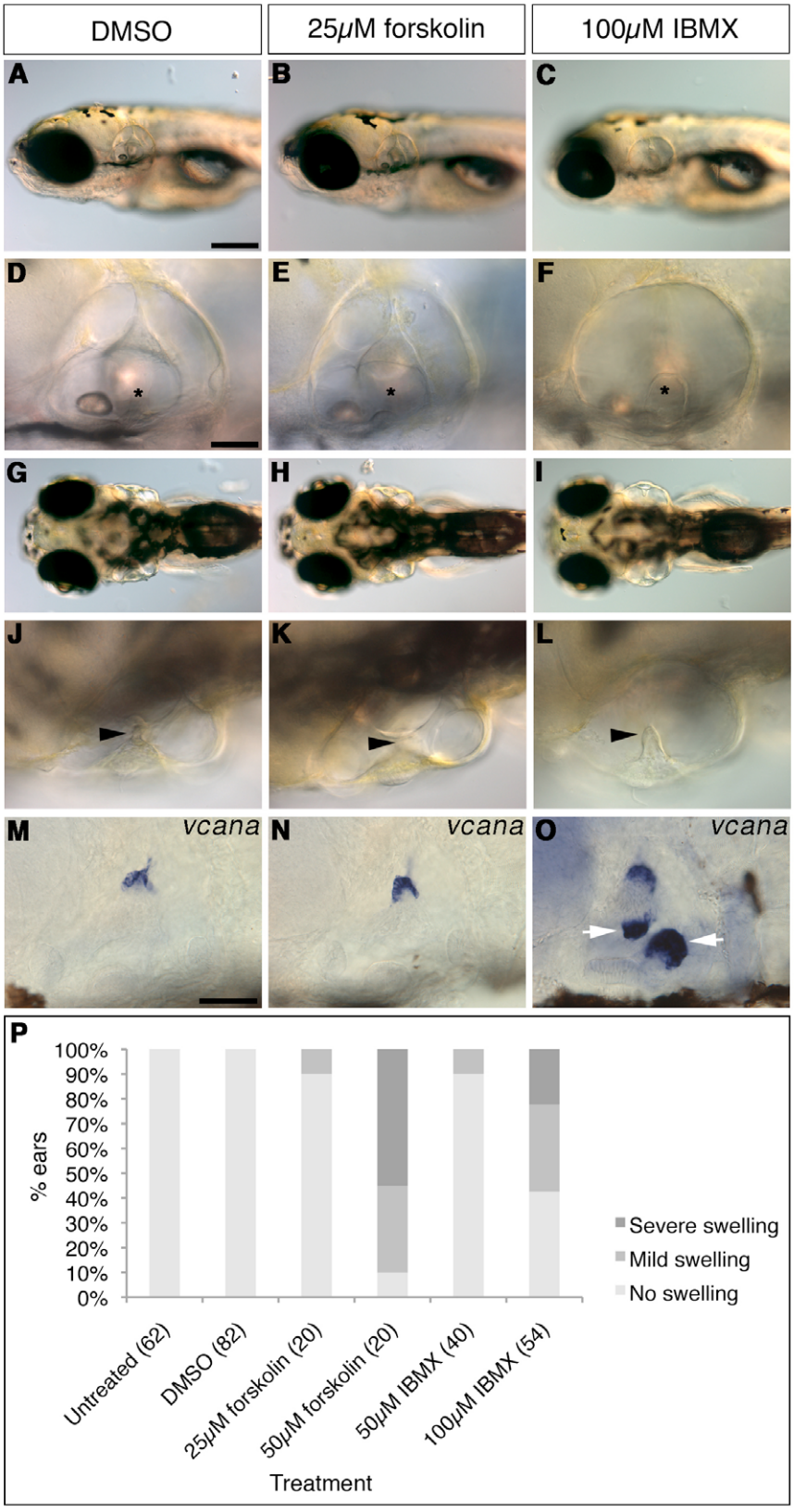

Figure S7. Treatment of wild-type embryos with cAMP agonists results in semicircular canal projection defects. (A-L) Live DIC images of 5dpf wild-type embryos incubated with DMSO, 25μM forskolin or 100μM IBMX between 60 and 90hpf show a gradation in phenotype. A low dose (25μM) of forskolin has little effect on the ear (B,E,H,K). However, treatment with 100μM IBMX can give rise to a severe phenotype, with a swollen ear and unfused projections (C,F,I,L). This is similar to the 'severe' category for the *tb233c* allele, but the swelling is not as extreme as in *tk256a* or *fr24* mutants. The dorsolateral septum (black arrowheads, J-L) and the ventral pillar (asterisks, D-F) have failed to form correctly in the presence of 100μM IBMX. **(M-O)** In situ hybridisation shows an upregulation of the ECM marker *vcana* in unfused canal projections (white arrows, O). Lateral views. Scale bars: A-C, G-I 200μm; D-F, J-L, M-O 50μm. **(P)** Graphical representation of the dataset. Ears swell as a graded response to both forskolin and IBMX concentration. Data were analysed with a 3×3 chi-square contingency table for each drug; $P<0.001$ for both drugs. *N* numbers are shown in parentheses.

Table S1. List of *in situ* hybridisation marker genes, primer sequences and morpholino sequences

Gene	ZFIN ID	Reference
aldh1a3	ZDB-GENE-061128-2	(Pittlik et al., 2008)
atp1a1a.4	ZDB-GENE-001212-4	(Blasiole et al., 2006)
bmp4	ZDB-GENE-980528-2059	(Hammerschmidt et al., 1996)
bmp7b	ZDB-GENE-060929-328	(Shawi and Serluca, 2008)
chsy1	ZDB-GENE-030131-3127	(Thisse and Thisse, 2004)
eya1	ZDB-GENE-990712-18	(Sahly et al., 1999)
fgf8a (fgf8)	ZDB-GENE-990415-72	(Reifers et al., 1998)
foxi1	ZDB-GENE-030505-1	(Solomon et al., 2003)
gpr126	ZDB-GENE-041014-357	This work: the *gpr126* probe used was a 4.6 kb cDNA clone covering the full open reading frame. The cDNA was cloned into the pCRII-TOPO vector, digested with *Not*I and transcribed with SP6.
hapln1a	ZDB-GENE-050302-175	(Kang et al., 2008)
hapln3	ZDB-GENE-040426-2089	(Thisse and Thisse, 2004)
has3	ZDB-GENE-021118-1	(Bakkers et al., 2004)
kcnq1	ZDB-GENE-061214-5	(Abbas and Whitfield, 2009)
mbpa	ZDB-GENE-030128-2	(Brösamle and Halpern, 2002)
pax2a	ZDB-GENE-990415-8	(Pfeffer et al., 1998)
slc12a2 (nkcc1)	ZDB-GENE-040625-53	(Abbas and Whitfield, 2009)
sox9b	ZDB-GENE-001103-2	(Chiang et al., 2001)
tbx1	ZDB-GENE-030805-5	(Piotrowski et al., 2003)
ugdh	ZDB-GENE-011022-1	(Busch-Nentwich et al., 2004)
vcana	ZDB-GENE-011023-1	(Kang et al., 2004)
vcanb	ZDB-GENE-030131-2185	(Kang et al., 2004)

Primer sequences for genotyping

Genomic DNA was amplified using the following primers flanking the mutations: for *tb233c* and *tk256a*, forward 5'-GATGAATCTCAGCACATCACTGC-3' and reverse 5'-GGTCAGTTTGAACTTCATGAGC-3'; for *fr24*, forward 5'-ACTTTGCAAGTACACGTCAGC-3' and reverse 5'-ATTGTCACTGTAAAGCATGCCA-3'.

Morpholino sequences

Gpr126 splice site morpholino: 5'-ATGCTGAAAGACACTCACTCAAAAG-3'

Control 5-base mismatch morpholino: 5'-ATcCTGAAAcACAgTgACTgAAAAG-3'